Fast Breeder Blanket Facility

NP-1657
Research Project 514-1

Interim Report, January 1981

Prepared by

PURDUE UNIVERSITY
School of Nuclear Engineering
West Lafayette, Indiana 47907

Edited by
F. M. Clikeman

Prepared for

Electric Power Research Institute
3412 Hillview Avenue
Palo Alto, California 94304

EPRI Project Manager
B. R. Sehgal

Developing Applications and Technology Program
Nuclear Power Division

ORDERING INFORMATION

Requests for copies of this report should be directed to Research Reports Center (RRC), Box 50490, Palo Alto, CA 94303, (415) 965-4081. There is no charge for reports requested by EPRI member utilities and affiliates, contributing nonmembers, U.S. utility associations, U.S. government agencies (federal, state, and local), media, and foreign organizations with which EPRI has an information exchange agreement. On request, RRC will send a catalog of EPRI reports.

NOTICE

Prepared by
Purdue University
West Lafayette, Indiana

EPRI PERSPECTIVE

PROJECT DESCRIPTION

The work in RP514-1 consisted of designing, constructing, and licensing (for operation) a fast breeder blanket facility (FBBF) at Purdue University in Lafayette, Indiana. The facility is employed to conduct experiments on prototypical blanket compositions and configurations to measure physics parameters of interest.

PROJECT OBJECTIVE

The major objective of this EPRI-sponsored project was the designing, constructing, licensing, and commissioning of a new facility in the U.S. for liquid metal fast breeder reactor (LMFBR) research. The facility is specifically designed for research on LMFBR blankets. This project was conducted in cooperation with a project sponsored by the U.S. Department of Energy (DOE); the principal aim was and is to pursue an extensive experimental research program on various blanket compositions and configurations. The objective is to reduce the uncertainties in the prediction of blanket physical behavior during the course of its life in the reactor. The work is related to the extensive research pursued by DOE in physics design of LMFBRs.

PROJECT RESULTS

The project work has been successful in fulfilling its objective. The FBBF has been employed in generation of (1) neutron reaction rates, (2) gamma energy absorption rates, and (3) neutron spectrum data at various locations in a prototypical LMFBR cylindrical blanket with natural uranium fuel rods.

The facility was designed, constructed, licensed, and commissioned essentially within the assigned budget, although with a delay in schedule. It has been operating successfully since its commissioning. The experimental research program is continuing and will include radial variation of the blanket compositions. The results are reported in quarterly reports published by DOE, Chicago operation's office.

The work reported here should be of interest to the experimenters and designers who work on blankets for fast breeder power reactors.

B. R. Sehgal, Project Manager
Nuclear Power Division

ABSTRACT

The Fast Breeder Blanket Facility (FBBF) located at Purdue University is a subcritical facility designed to investigate the neutron and gamma-ray physics of the blankets of fast breeder reactors (FBR). The facility was designed to mock-up, using UO_2 fuel rods, the blanket regions of FBR's. The facility, using a cylindrical geometry and an isotopic neutron source, drives the experimental blanket region with a neutron flux that has an energy and spatial dependence similar to a 1000 MW_e FBR. Measurements of the neutron reaction rates, both capture and fission, neutron energy spectra, and gamma-ray absorption rates as a function of position in the blankets can be measured and then compared with calculated values.

This report contains a summary of the philosophy and design considerations in the facility. Since the facility was to be built and operated at a university, special safety considerations had to be factored into the design. The report also contains a detailed description of the facility together with a summary of criticality calculations that were made to insure the safety of the facility under both normal and accidental flooding conditions. A summary of the measurements of k_{eff} and the shielding, as required by part of the license conditions are also presented. Finally, samples of some of the preliminary experimental measurements are presented.

$\leq$.

CONTENTS

LIST OF FIGURES

LIST OF TABLES

SUMMARY

This report summarizes the details of the design philosophy, constraints, construction details, safety calculations and preliminary measurements of the Fast Breeder Blanket Facility (FBBF) located at Purdue University.

With projected future shortages of uranium, the role of the fast breeder reactor is becoming increasingly important in future nuclear energy programs. Much of the breeding, or production of fissile fuel from fertile materials such as U-238, will be done in blankets, or regions surrounding the central core of the fast reactor. To date, most of the experimental physics research has been concerned with the core of the fast reactor. For the core region, there are a number of good bench mark type experiments for the verification of the computer codes that will be used in the design of the new reactors. However, at present, there are no experiments for the verification of cross sections and calculational methods to be used in the design of the blanket regions of the fast reactors. In the blanket regions, where the energy dependence of the neutron flux varies with position, a number of the calculation methods used in the core regions are no longer expected to be valid.

The Purdue FBBF facility has been built to mock-up the blanket regions of fast breeder reactors. Preliminary calculations showed that a subcritical facility using isotopic neutron sources and a converter region of low enriched uranium can be used to drive a blanket region with a neutron spectrum having the same energy dependence as the neutrons leaking from the core into the blanket regions of a commercial size fast reactor.

The initial blankets in the FBBF will consist of natural UO_2 fuel rods with aluminium cladding. Each fuel rod has a secondary clad or sleeve material also. By the use of secondary cladding material and adjusting the spacing of the fuel rods the number densities of the blanket can be adjusted to the same values that are being used in the current design of fast reactors, with the exception of the sodium coolant. No sodium is used on FBBF blankets, but the aluminum clad of the fuel rods serves as an approximate substitution.

The fuel rods are in a simple hexagonal pitch to make the calculations simpler. Future blankets will include the grouping of the fuel rods into hexagonal subassemblies that will mock-up the actual blanket design even closer. The use of the

subassemblies will introduce additional heterogeneities that will complicate the theoretical analysis of the blankets. Future blankets will also use low enriched uranium oxide fuel to simulate the buildup of the bred plutonium in the blanket.

Measurements made in the FBBF include various neutron capture rate measurements such as $^{238}U(n,\gamma)$, $^{232}Th(n,\gamma)$, $^{198}Au(n,\gamma)$ etc. as well as fission rates such as $^{235}U(n,f)$, $^{238}U(n,f)$, $^{239}Pu(n,\gamma)$, and $^{237}Np(n,f)$. A number of these reactions are the reactions expected in the blanket while the other reactions will give addition information on the nutron processes and provide addition tests of the calculation methods in different neutron energy regions. In addition, neutron spectrum measurements as functions of position in the blanket will be made using proton recoil proportional detectors. Gamma-ray energy deposition in the blanket regions will also be made as a function of position using thermolumine cent dosimeters. Examples of all of these measurements are included in the report.

I. INTRODUCTION

THE IMPORTANCE OF BREEDING

Nuclear fission will have to play an important role in providing energy for industrialized and developing countries. The only naturally found fissile material, ^{235}U, occurs with 0.7% in natural uranium. Therefore, relatively high grade uranium ore is needed to produce power from reactors which use ^{235}U. High grade ore is in short supply, but the "fertile" isotopes ^{238}U and ^{232}Th are found in abundance. Thus, large scale production of nuclear energy, over a period of many decades, requires the fissioning of fertile materials, either directly or after conversion of fertile nuclei into fissile ones. This conversion is technically realized in "converter reactors" (e.g., LWR; D_2O moderated reactors such as the CANDU; or high temperature gas cooled reactors). Converter reactors can stretch the uranium supply by recycling the generated fissile material. However, only through breeding, i.e., through enhanced conversion, such that at least as many fissile nuclei are produced as are consumed for the conversion, can the abundant fertile material provided energy on a world scale for centuries.

The currently best developed technical realization of the breeding process is in the fast breeder reactor, (FBR), especially its sodium cooled version (often called LMFBR, Liquid Metal Fast Breeder Reactor). An FBR consists of a "core" in which most of the power and most of the neutrons are produced and of a blanket, surrounding the core, in which a substantial part of the breeding occurs.

Other breeding systems are under investigation and have good technical prospects; e.g., an FBR with a thorium blanket or a fusion reactor with an uranium or thorium blanket. The Purdue Fast Breeder Blanket Facility has been built for researching, in a close mock-up, the physics of neutrons and γ-quanta fields in various blanket configurations. This information will provide the basis for more efficient design and operation of FBR and fusion reactor blankets.

The need for substantial additional research on fast reactor blankets was recently pointed out in a special report by the Nuclear Energy Agency Committee on Reactor Physics under the title "The Present Status of Fast Reactor Physics;" Chapter IV of this report covered "Blanket Physics."

The first series of blanket configurations will address uranium fueled blankets; at a later time, thorium fueled blankets could be considered. In thorium fueled blankets, ^{233}U is produced which can be used as light water reactor (LWR) fuel. Supply of ^{233}U by FBRs then allows the installation and operation of LWRs to continue for centuries.

For the study of fusion reactor blankets, the facility needs to be modified.

INACCURACIES IN BLANKET PHYSICS

Most of the experimental and theoretical neutron physics efforts in the U.S. Liquid Metal Fast Breeder (LMFBR) development program have been concerned with the performance and design problems of the cores in the fast reactors. Relatively little emphasis has been given to the blankets. Consequently, the inaccuracies in the presentation of the neutron and γ-quanta spectrum and distributions are much larger in blankets than in cores. The subsequent discussion of the reactor physic uncertainties is based on the respective Section in the Proposal for this project as originally submitted to ERDA and EPRI.

The studies on the ZPR and ZPPR critical assemblies of the Argonne National Laboratory have mocked-up the reactor cores (or benchmark cores) in great detail but not the blankets. In fact, UO_2 fuel platelets have not been used in blanket regions of the reactor mock-ups assembled on the ZPPR facility before 1972 (1). The only operating U.S. fast reactor, the EBR-II has had its inner four depleted uranium metal blanket rows changed to a stainless steel reflector (2). The Fast Test Reactor [FTR (3)] is designed to have a nickel-rich reflector and also the SEFOR (4) reactor did not contain a blanket. Thus, there is not enough experimental information available on the spatial distributions of neutrons, γ's and the power density as well as on the neutron and γ spectra in realistic fast reactor blankets. The available information from the ZPR and ZPPR experimental programs also suffers from the heterogeneity effects present in the platelet geometry of the blanket mock-up compositions.

Theoretical studies on accurate predictions of neutron, γ and power distributions in fast reactor blankets are confronted with the difficulty of transition nature of the neutron spectra existing in the rather thin ($\cong$ 40 cm thick) radial (or axial) blankets. The radial blanket adjoins the core and the thermal-shield (reflector) regions which have different compositions from that of the blanket; therefore, an equilibrium neutron spectrum does not exist in the blanket. The methods of calculation based on utilizing fine group equilibrium spectra for generating broad group neutron cross sections for blankets [as in the MC^2 Code (5)] have led to poor comparisons with reaction rate distributions measured in reactor blankets. Also the ^{238}U capture rate and the power distributions in the reactor blankets have not been predicted as accurately as in the core regions. The uncertainties in the ^{238}U capture rate distribution affect those in the blanket power distribution increasingly with reactor operation as the bred plutonium starts producing larger and larger fractions of the power generated in the blanket. Improvements in these predictions can be expected from the newer methods [SDX (6)] which employ transition spectra for the broader group constant collapsing.

The evaluation effort on neutron cross section to generate data files for reactor calculations, e.g., the ENDF/B Versions I, through IV have also been geared towards improving calculated predictions in the core region of the fast reactors. Thus, for example the new ENDF/B versions are tested against measured data for criticality, reaction rate ratios (at core center) and material worths on a set of critical assemblies. The improvements achieved in predicting core physics-parameter measurements by cross section improvements have not always brought greater success in predicting the blanket physics-parameter measurements (7). Little information is available on thorium in fast reactor blankets, and on the thorium cross sections in typical blanket spectra.

Fast reactor blankets generate a considerable fraction of their power due to absorption, since the γ source from the reactor core is preferentially absorbed in the blanket. The prompt and delayed γ rays carry about 14% of the energy generated in fission and their spatial absorption-energy distributions do not follow the spatial fission distributions. Measurements of γ-ray absorption-energy have been performed with Thermoluminescent detectors (TLD's) in ZPPR assemblies (8) and in EBR-II criticals (9,10). The confidence in the measurements with the TLD's and the γ energy deposition calculations based on a set of

γ production and transport cross sections needs to be improved. There is a need for measurements of γ-ray magnitudes, spectra and spatial distributions in the blankets of fast reactors. Unfortunately, such measurements are plagued by the high background due to the $^{238}U(n,\gamma)$ reaction and the natural activity of uranium in the blanket.

The uncertainties in the time-dependency (over the blanket fuel-cycle time) of the blanket power magnitude and spatial distributions may force reactor dsigners to overcool the blankets and not obtain the desired reactor coolant outlet temperatures. The loss in plant efficiency may become quite an economic penalty during the long-term operation of a fast reactor. The uncertainties in the temperature distribution create problems for the reactor designers in terms of the uncertainties in the resultant thermal stresses and deflections.

THE PURDUE FAST BREEDER BLANKET FACILITY, FBBF

The Purdue Fast Breeder Blanket Facility, FBBF, has been built to allow--through appropriate research--a sizable reduction of the uncertainties described above. The results will provide the basis for a more efficient design and operation of fast breeder blankets with uranium or thorium fuel. No plutonium is needed for the mock-up of a blanket. Furthermore, the blanket itself is not a reactor, neither is the small converter region in which the neutron spectrum is adjusted to match the spectrum in a reactor. Neutrons are provided by a radioactive source. Therefore, a blanket mock-up facility is a safe system and can be built and operated on a university campus.

In this report, the basic design features, the typical neutronics characteristics and the experimental capabilities are described (Sections III, IV, and VI). Safety considerations are presented in Sec. V. First results are shown in Sec. VII.

The research to be conducted with this facility is of high educational value. A special dual-level laboratory course is being devised to allow for a much broader utilization of the FBBF in undergraduate and graduate education.

ACKNOWLEDGEMENTS

The planning, design and building of the Purdue Fast Breeder Blanket Facility was only possible through the strong and continuous encouragement, help, and support by many:

The former AEC Division of Nuclear Education and Training (DNET) strongly encouraged us to pursue a project of this kind. The DNET, now part of the Department of Energy (DOE) provided the necessary uranium dioxide fuel rods on a loan basis; about 11,000 UO_2 rods of various enrichments (4.8%, 1.3% and natural uranium) have been obtained on loan. In addition, the acquisition of the fuel and further planning of the facility had been supported by a $12,250 grant by the same agency. Specifically acknowledged is the help of Dr. R.J. Neuhold in locating the needed types and quantities of fuel rods in various surplus stockpiles.

Several utilities encouraged us to forcefully proceed with this project because of its importance for long-term efficient generation of electrical power; among them Commonwealth Edison, Public Service Indiana, Consumers Power, Detroit Edison, and Cincinnati Gas and Electric.

A $3,000 grant by Gulf General Atomics supported some of the design work. The bulk of the detailed design work and the construction has been supported by the Electric Power Research Institute, EPRI under RP-514 . Most of the instrumentation has been purchased from funds received from Purdue University ($50,000) and from Purdue Electric Power Center, PEPC ($20,000). The first research phase, including most of the preparatory research and the work needed for the license has been supported in part by the Department of Energy (DOE, formerly ERDA) with a research contract in the amount of $414,585.00. Furthermore, DOE also provided the neutron source (^{252}Cf) on a loan basis.

A precondition for this project was the interest and the cooperation of the Purdue University Administration, especially of Dean John C. Hancock. Administratively, the financial-support, the contract-negotiations, and the construction phase were the most difficult phases. The continued and intensive cooperation of Professor Paul S. Lykoudis, Head of the School of Nuclear Engineering, was vital for this project during these phases. The realization of the FBBF project is

largely due to his intensive help and effort in finding the needed support and solving all administrative problems.

Special thanks is due to the Physical Plant and the Central Machine Shop of Purdue University for their excellent cooperation in the design and construction of the facility; Mr. Tom Bennett and Mr. Charles Schenke are thanked for their numerous suggestions in improving the facility design.

Several former and current students of the School of Nuclear Engineering contributed significantly to the early feasibility studies (C.W. Terrell), the conceptual design (F.G. Krauss), the safety, neutronics and shielding investigations (L.L. Luck, K.R. Boldt, D.J. Malloy, J.E. Arpa, D.W. Vehar, J.L. Westbrook, J.A. Maniscalco, and P.J. McDaniel).

II. DESIGN CRITERA
(F.M. Clikeman)

The purpose of the Purdue Fast Breeder Blanket Project is to design, construct, and operate a small, flexible facility in which the blankets of fast reactors could be mocked-up and measurements made for the study of the neutronic and gamma-ray transport processes. The facility, called the Fast Breeder Blanket Facility or FBBF, is to mock-up the blanket regions in a realistic geometric configuration and material arrangement. Zero power, critical facilities, such as ZPR and ZPPR, use platelets, placed in drawers, to mock up the material composition of the core and blanket regions of fast reactors. The heterogeneity effects of the platelets are not important in the core but introduce large errors in the softer neutron spectrum of the blanket regions. Other facilities, designed to mock-up fast reactor blankets, have been constructed using a slab geometry which introduces a geometry correction that often masks the phenomena being measured.

The following criteria were established for the design of the FBBF:

1. --The geometry of blanket should be cylindrical so that the same computer codes and geometeries that are being used in the design of fast reactors may be used to analyze the blankets in the FBBF.

2. --The material in the blanket should match as closely as possible, both in the number density and physical shape, the materials in fast reactor blankets.

3. --The neutron spectra driving the blanket region should match, as nearly as possible, the neutron spectra leaking from the core into the blankets of fast reactors.

4. --The neutron flux strength in the blanket should be strong enough to provide meaningful measurements of neutron and gamma transport phenomena and reaction rates for comparison with analytical results.

5. --The facility should be safe for operation on a university campus

The above criteria led to a number of early design decisions first supported in a paper by Ott and Terrell (11). The first important decision was the use of a

cylindrical facility driven by either a neutron generator or isotopic neutron source in the center or along the central axis of the cylinder. Surrounding the neutron source is a converter region consisting of low enriched uranium to modify the source neutron spectrum to a spectrum typical of that leaking out of the core of a fast reactor. Ott and Terrell showed that by varying the composition and radius of the converters, that the energy spectrum as well as the spatial dependence of the neutron flux driving the blanket regions can be made to match the neutron flux in the blanket of fast breeders. Further investigations lead to the choice of ^{252}Cf as the preferred neutron source.

A second early decision lead to a compromise on the materials to be used in the mock-up of the blankets. Because of the cost of fabricating nuclear fuels, the project was limited to using fuel rods that were already fabricated and available from various government projects. This surplus nuclear fuel included stainless steel clad, 4.8% enriched UO_2 fuel for use in the converter regions, and aluminum clad 1.3% and natural UO_2 for use in the blanket regions. Since aluminum is not found in the blankets of fast reactors, a compromise had to be made in the composition of the blanket mock-ups. The decision was made to use correct number densities for the UO_2 and stainless steel in the blanket, but not to use sodium. Instead, since aluminum was present as the fuel cladding, the effects of the sodium in the blanket was to be simulated by the aluminum, however, no attempt would be made to match the number densities or macroscopic cross sections of the aluminum to the sodium.

The basic philosophy governing the design of experiments in the FBBF is two fold. First, the experiments should yield information useful in verifying and improving the calculational methods used in the blanket regions of fast reactors. Second, the experiments should yield some basic data or provide a means of evaluating basic nuclear data used in theoretical calculations. It is expected that with a systematic program of experimentation and analysis a capability of improved predictions of important parameters for design and operation of fast reactor blankets can be achieved. Within the guidelines of this general philosophy, three general types of experiments were planned for the FBBF.

The first broad category of experiments is the systematic comparison of experimental activation and reaction rate data with theoretically calculated activation and reaction rates throughout the blanket region. Early sensitivity studies (12, 13) indicated that most important reaction rates such as $^{238}U(n,\gamma)$, $^{235}U(n,f)$,

$^{238}U(n,f)$ and $^{239}Pu(n,f)$ could be measured in the FBBF blanket mock-ups using a driving source emitting between 10^{10} and 10^{11} neutrons per second. The sensitivity studies considered the anticipated experimental uncertainty as well as the uncertainties in the neutron cross sections used in the calculations. In each case, the experimental method deemed best suited to the FBBF facility was used as the basis for the calculations. In the case of the $^{238}U(n,\gamma)$ reaction several experimental methods of measurement were considered in order to find the technique best suited for the FBBF. Two different techniques are being used to determine the neutron reaction rates. The first technique is the activation of foils followed by the measurement of the foil activities. Among the more important activities included in this technique is the ^{239}Np activity from the irradiation of ^{238}U foils since this is a direct measurement of the ^{239}Pu breeding rate. The second technique is the use of solid state track recorders (SSTR) for the measurement of the fission rates of ^{235}U, ^{238}U, ^{237}Np, ^{239}Pu and ^{232}Th. The ^{238}U and ^{239}Pu fission rates will give important information about the blanket fission rates and, hence, the heat generation rate in fast breeder blankets. These two fission rates together with the ^{235}U, ^{237}Np and ^{232}Th fission rates provide information on the energy dependence of the neutron flux.

A second broad category of experiments is the determination of the energy dependent neutron flux in the blanket. Again, two different techniques were planned so as to have an independent check on the measurements. The primary method is the use of proton recoil neutron spectroscopy to determine the neutron spectra. The neutron spectra will be compared with spectra determined from the computer code SAND-II, (14) and CRYSTAL BALL (15) using the foil activation and fission rates as input. Both of these experimentally determined spectra will be compared with the theoretically calculated spectrum providing another check of the calculational tehcniques and basic assumptions used in the computer codes.

The third main category of experiments involves the use of thermoluminescent dosimeters for the measurement of gamma heating. This information will contribute to a better understanding of the spatial dependence of the heat generation in the breeder blankets.

Combined, these experiments will form a large pool of information for comparison with theoretical calculations. The comparison will either serve to veryfy calculational techniques and the basic nuclear data for the blanket and shield-type materials or will point out areas where improvement is needed. In addition, the

experiments will provide accurate information concerning the distribution of plutonium breeding, fission rates, and gamma heating throughout the blanket as well as information on the neutron spectrum emerging from the breeder blanket.

Early safety considerations for a fast breeder blanket subcritical facility for use on a university campus had ruled out the use of plutonium because of the hazards and extreme care that must be exercised in its handling. Subsequent studies led to the conclusion that typical neutron spectra could be obtained without plutonium by using enriched uranium in the converter regions. Additional consideration including the possibility of an accidental criticality in the event that the facility were flooded led to a series of criticality investigations to insure that ll of the proposed blanket mock-ups would remain subcritical by a safe margin. Operational procedures were developed to insure the safe handling of the fuel during transfer between storage areas and into and out of the facility. The third area of safety concern was adequate shielding around the facility to minimize the radiation exposure to the operating personnel and the rest of the university community, especially the students. This latter safety concern became especially important because of the close proximity of two large lecture halls in the same building. The shielding design, besides providing adequate protection, also had to provide ready access to the facility to permit changing experiments and blankets.

Based on the above criteria, a series of studies were initiated that culminated in the design of the Purdue Fast Breeder Blanket Facility with an initial source strength of 10^{10} neutrons per second. Details of the facility and it's construction, neutron spectrum matching calculations, criticality calculations, shielding performance measurements and preliminary measurements are given in the following sections of this report.

3

DETAILED DESCRIPTION OF THE PURDUE UNIVERSITY FAST BREEDER BLANKET FACILITY

(P.J. Fulford, F.M. Clikeman and R.H. Johnson)

GENERAL

(P. J. Fulford)

The laboratory consists of an experimental assembly located inside a shielded room (Room B28C) which is in turn situated inside a large facility room (Room B28). Associated with the facility (see Figs. 3-1 and 3-2) are various pieces of experimental equipment, operational and experimental instrumentation and some service facilities.

THE EXPERIMENTAL ASSEMBLY (Spring 1978 CONFIGURATION)

The assembly consists of a pseudo-line source of fast neutrons, a set of two concentric annular cylinders containing enriched uranium and some sodium to transform the source spectrum, the annular blanket (experimental) region surrounded by a reflector, an upper blanket, a source drive mechanism, a source storage cask, and associated structural components. The assembly is shown in Fig. 3-3. A detailed description of each of these components is given below. Subsequent sections describe the shielding and the laboratory facilities.

SOURCES AND SOURCE TUBE

The four sources are doubly-encapsulated ^{252}Cf sources, ORNL model NSD, positioned in a tube to represent a pseudo-cosine line source. The source capsules are stainless steel and are illustrated in Fig. 3-4.

The source tube is 316 stainless steel tube 12.95 mm (0.510 in.) inside diamter and 25.4 mm (1 in.) outside diameter with a shielded lower hemispherical cap. The lower cap has a cross bar on its lower surface that matches a slot in the source receptacle in the storage cask. The upper end of the tube has an enlarged 35.5 mm (1.40 in.) diameter, is threaded, and has two wrench flats. A soft copper ring sits in a sealing surface on the upper end. A cap screw makes the seal. This top cap was screwed and peaned into place at Oak Ridge National Laboratory, producing a triple-encapsulated source assembly.

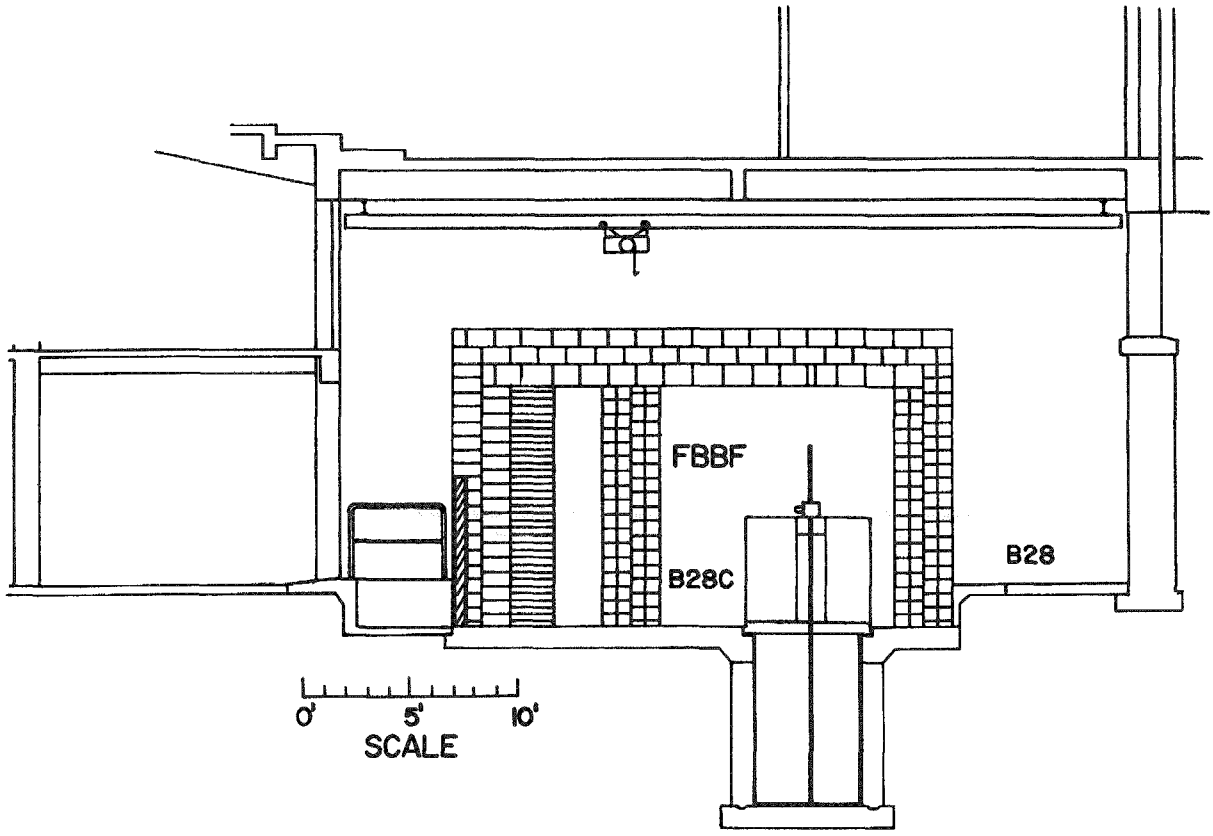

Figure 3-1 : Cross-sectional view of the FBBF laboratory showing the FBBF inside the concrete blockhouse (Room B28C).

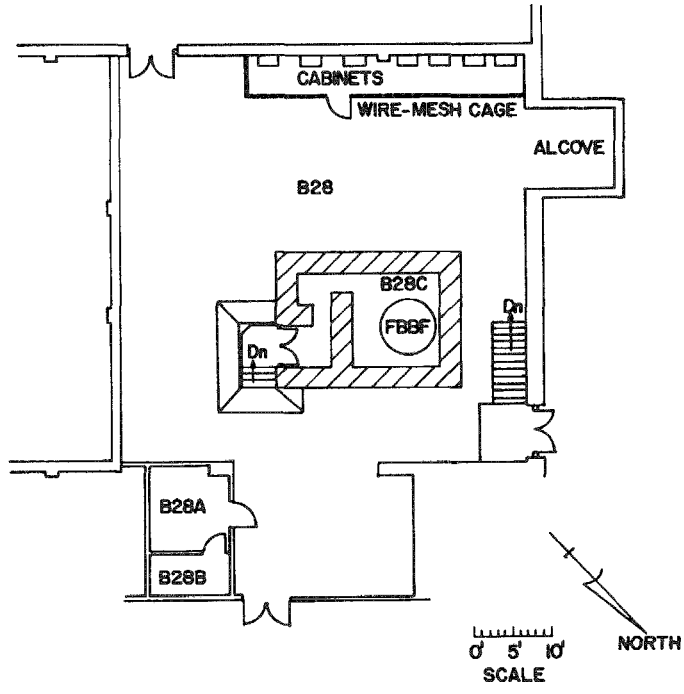

Figure 3-2: Floor plan of the FBBF laboratory.

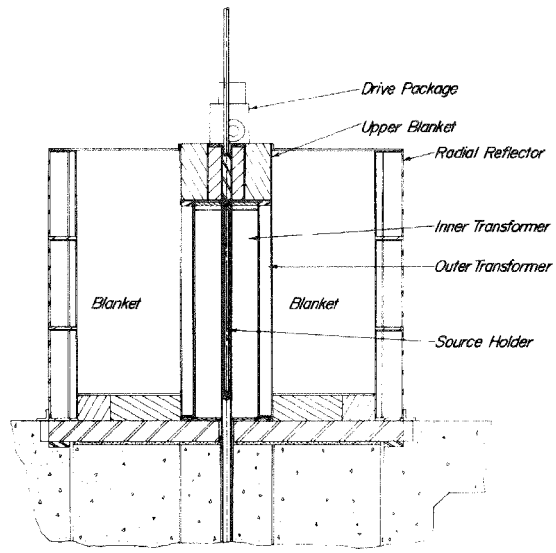

Figure 3-3: Cross-sectional view of the FBBF experimental assembly.

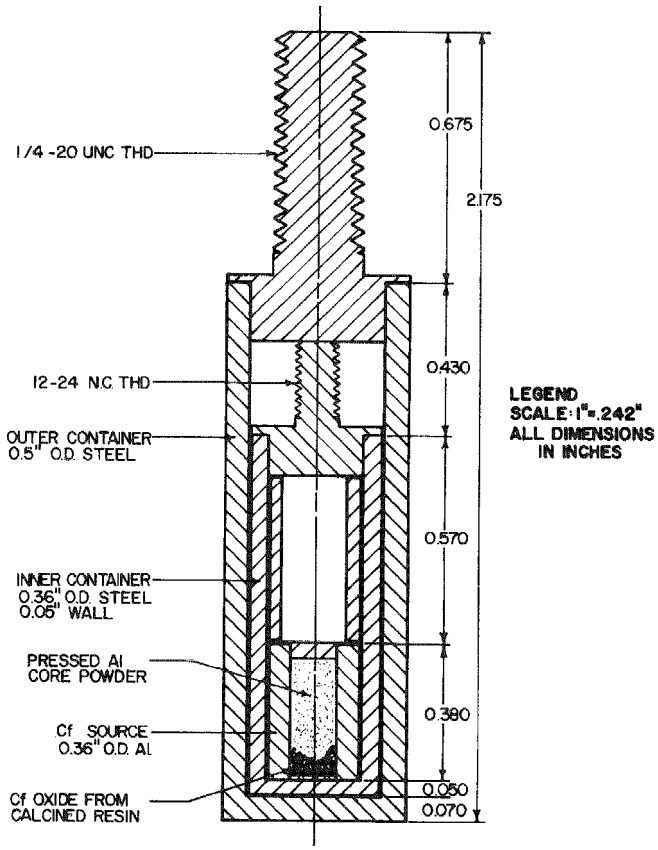

Figure 3-4: Source capsule.

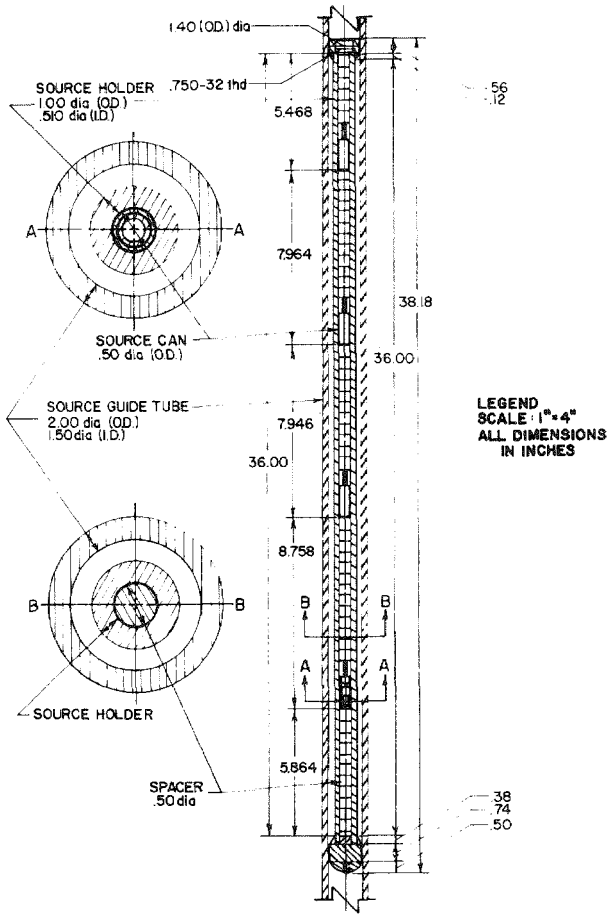

Figure 3-6 Drawing of the 2.54 cm (1") diameter neutron source holder with a cutaway section showing one of the double-encapsulated neutron source and the stainless steel spacers. The end of the source holder is sealed with a soft copper high vacuum type seal, producing a triple-encapsulated source assembly.

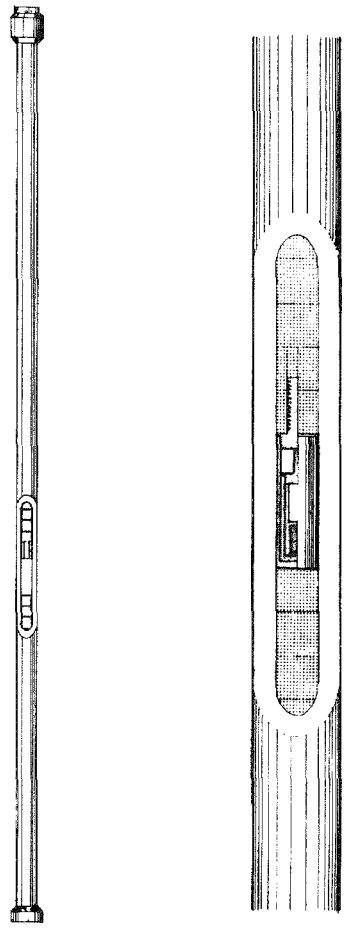

Figure 3-5: Source tube and source guide tube.

At the bottom end of the tube a small partially compressed coil spring supports the string of 316 stainless steel 12.7 mm (0.5 in.) diameter steel spacers and the source capsules. A similar spring is at the top of the string. The springs are to reduce any shock loads on the source capsules. The assembly including the capsule spacing is shown in Figs. 3-5 and 3-6.

SOURCE GUIDE TUBE

The source guide tube, Fig. 3-5, provides a smooth uninterrupted guide for movement of the source tube and its extension rod through the experimental assembly down to the middle of the source storage cask. It is a 316 stainless steel tube 38.1 mm (1.5 in.) inside diameter and 50.8 mm (2.0 in.) outside diameter. The inner diameter is honed to a 32 rms microfinish. The tube extends from the top of the upper blanket to the locating surface on the lower plug in the storage cask central pipe. It is held at its upper end by a screwed brass bushing which sits in the upper blanket can top plate. This bushing provides the physical stop against source overtravel. It is physically locked against removal by the source drive package (see Fig. 3-3).

INNER TRANSFORMER ZONE

This zone is contained in a welded 316 stainless steel annular cylindrical can. The can is 320 mm (12.6 in.) outside diameter, and 1.09 m (43 in.) high with a 58.9 mm (2.3 in.) diameter central through-hole. The can contains 528 of the 4.8% enriched pins located on a 12 mm (0.474 in.) tight triangular pitch by an upper grid plate in the can. The remaining space in the can is filled with B_4C packed in place. The packed density of the B_4C is 1.54 g/cm^{-3} and the loaded weight was 21.59 kg. The can is shown in Fig. 3-7.

The loaded can weighs approximately 670 kg. It rests on the base assembly and is located by pins concentrically to the facility vertical centerline.

The bottom plate of the cylinder is 12.7 mm (0.50 in.) thick and the top 19 mm (0.75 in.). The walls are 14 gauge.

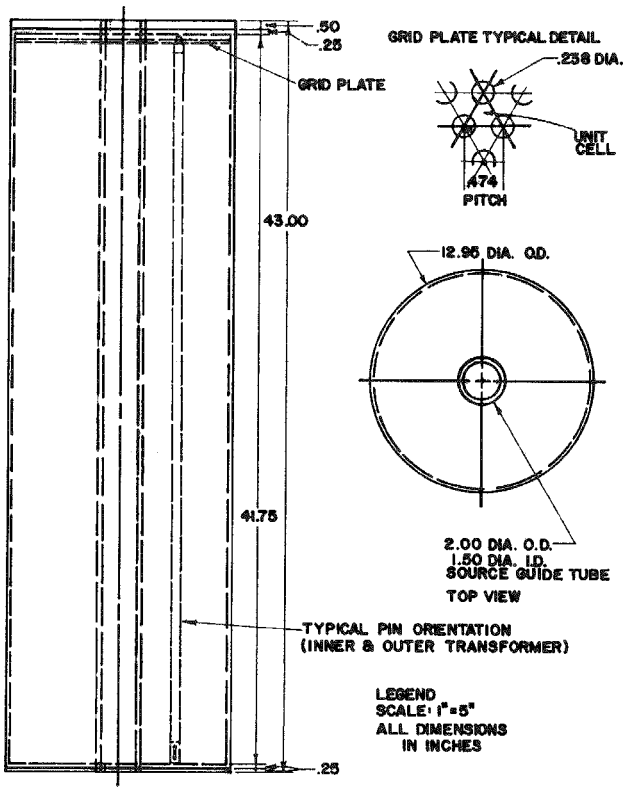

Figure 3-7: Inner transformer.

OUTER TRANSFORMER REGION

This zone is contained in a sealed stainless steel annular cylindrical can and is illustrated in Fig. 3-8. The inside annulus diameter is 320 mm (12.6 in.) and the outside diameter is 443 mm (17.45 in.). This zone contains an approximately circular zone of 4.8% enriched pins spaced on a 17.93 mm (0.706 in.) hexagonal pitch. Unequal-sided hexagonal-shaped 316 stainless steel pins containing frozen sodium are located between the fuel pins. There are 198 fuel pins and 396 sodium pins. The fuel pins are located by a 4.5 mm (0.187 in.) thick aluminum grid plate at the bottom. The balance of the space is filled with B_4C powder with a packed density of 1.33 g/cm^{-3}. Two 22.9 mm (0.90 in.) inside diameter experimental reentrant probe tubes are provided at a 180° spacing. They are accessable through 38.1 mm (1.5 in.) diameter plugs screwed into the top plate of the cylinder. A fuel pin or some sodium pins can be placed in these holes to minimize spectrum perturbations.

The cylinder weighs approximately 340 kg. It is 0.63 mm (0.25 in.) higher than the inner transformer can and thus supports the upper blanket. The can sits on the lower base plate assembly and is located by pins.

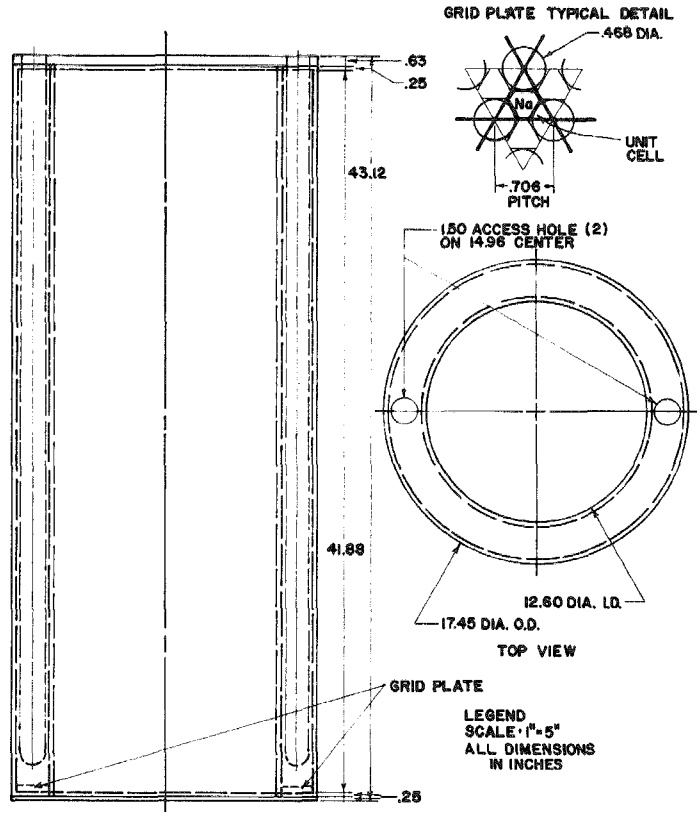

Figure 3-8: Outer transformer.

RADIAL BLANKET REGION

The radial blanket region is the annular volume between the inside of the radial reflector pans and the outside face of the outer transformer can. The lower surface is the top of the base plate assembly. There are 5994 15.2 mm (0.6 in.) diameter natural UO_2 pins located in this region on a 17.0 mm (0.67 in.) hexagonal pitch.

Six 60° segment 4.5 mm (0.187 in.) thick aluminum grid plates locate these pins at both their top and bottom ends. The lower grid plates are screwed to the base plate. The upper grid plates are screwed to the top of the reflector can and the upper blanket can. The bottom end of the fuel pin locates in the hole in the grid plate while an aluminum dowel pin locates the top of the fuel pin through the grid plate. The fuel pins have aluminum or stainless steel tubes, termed secondary cladding or filler tubes, over them for experimental purposes. A typical arrangement is shown in Fig. 3-9. The filler tubes are 15.29 mm (0.602 in.) ID, 16.97 mm (0.668 in.) OD by 1.238 m (48.7 in.) long. A small number of pins are removable for experiment access. At these sites the top grid plates are drilled out to the full pin diameter (plus a clearance).

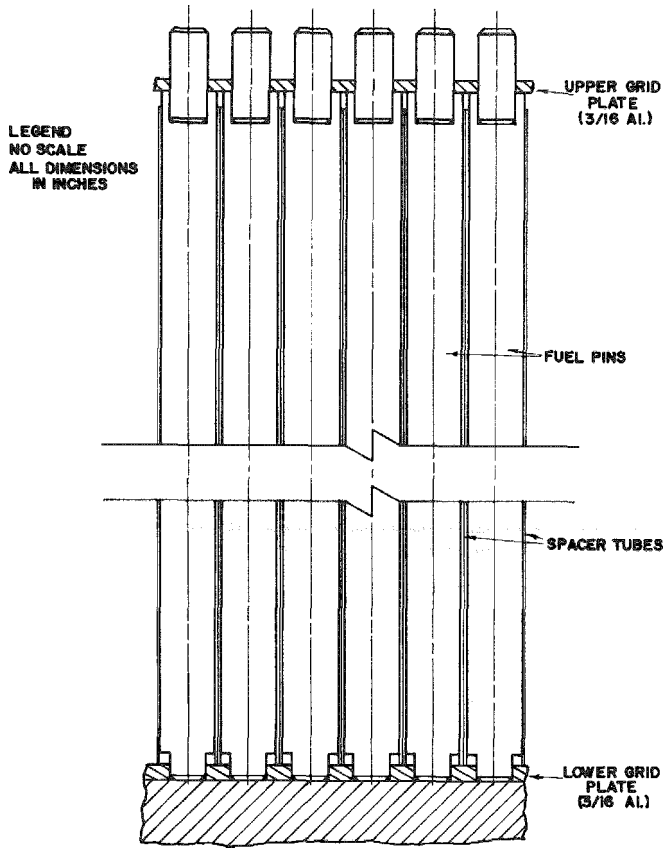

Figure 3-9: Typical arrangement of radial blanket fuel pins and secondary cladding.

REFLECTOR REGION

A nominal 152 mm (6 in.) thick annular zone composed of about two-thirds mild steel and one-third salt by volume surrounds the radial blanket region. The material is contained in 18 cans, each one-third of the zone height and 60° of the perimeter. The can is sectioned with the inner zone containing an average 21.8 kg (48 pounds) of salt and the outer zone containing six 12.7 mm (0.5 in.) thick curved mild steel plates. A typical can is shown in Fig. 3-10 . The cans are bolted together to form a continuous zone. Each can weighs on the average a total (salt and steel) of 329.5 kg (726 pounds).

UPPER BLANKET

The upper blanket currently provides shielding above the transformer region, supports the drive mechanism, locates the top end of the source guide tube, and supports the inner edge of the blanket upper grid plates. Access is provided to the top of the outer transformer region by two 144 mm (4.5 in.) diameter hand access holes. The blanket dimensions are 58.9 mm (2.32 in.) inside diameter,

443 mm (17.45 in.) outside diameter and 282.4 mm (11.12 in.) high. The blanket can is shown in Fig. 3-11 .

The upper blanket is essentially a welded 316 stainless steel can filled with lead. The bottom plate is 12.7 mm (0.5 in.) thick as are the top plate and the side walls. The lead has been cast in two layers, the bottom one being 203 mm (8 in.) thick, and the top 50.8 mm (2 in.). They are separated by a thin asbestos sheet. The bottom layer of lead can be replaced by 25.4 mm (1 in.) diameter natural U metal slugs currently available at Purdue.

The can weighs approximately 367 kg (810 pounds) and the lead plugs weigh 32 kg (70 pounds) each.

BASE PLATE ASSEMBLY

The base plate assembly consists of a number of steel plates laying horizontally across the top of the opening of the storage well. These plates support and locate the transformer cans, the radial blanket, and the reflector cans. They also provide gamma and neutron shielding between the source cask and the experimental assembly proper.

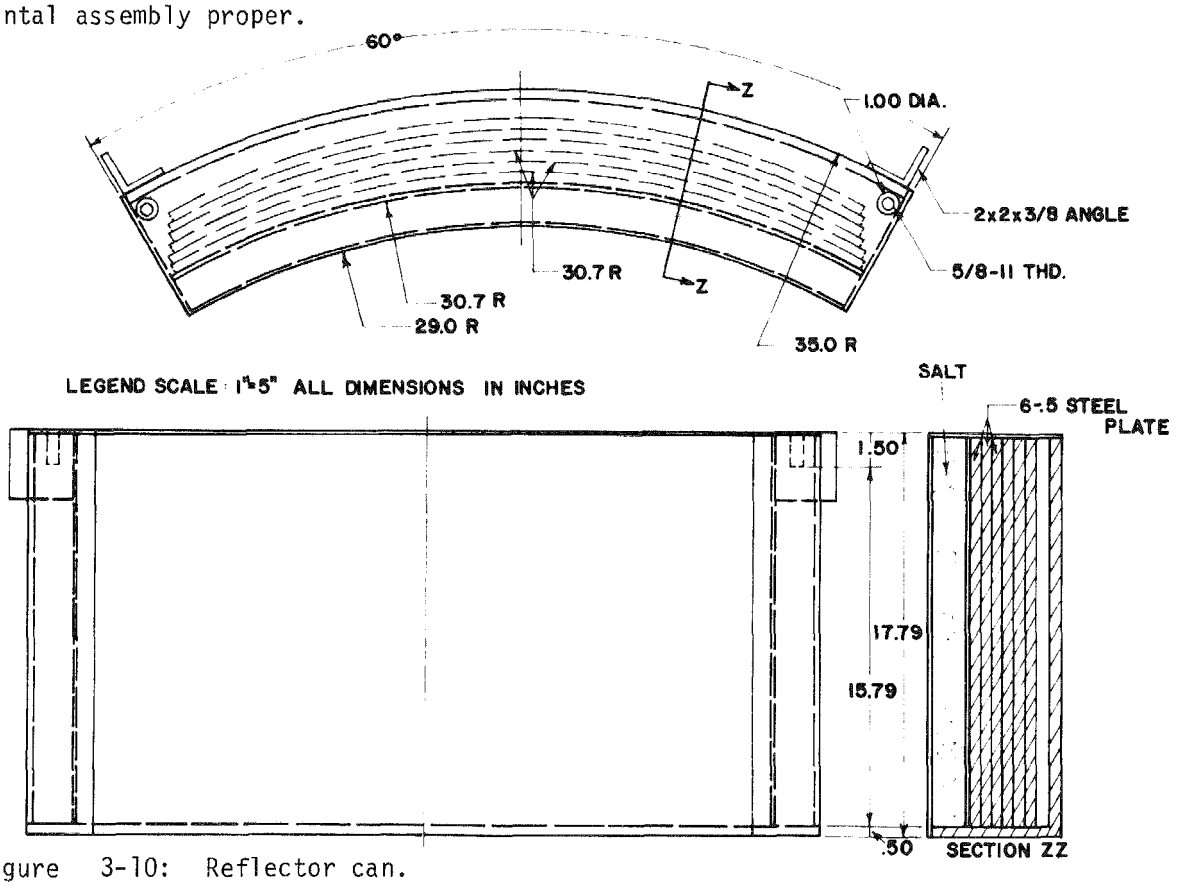

Figure 3-10: Reflector can.

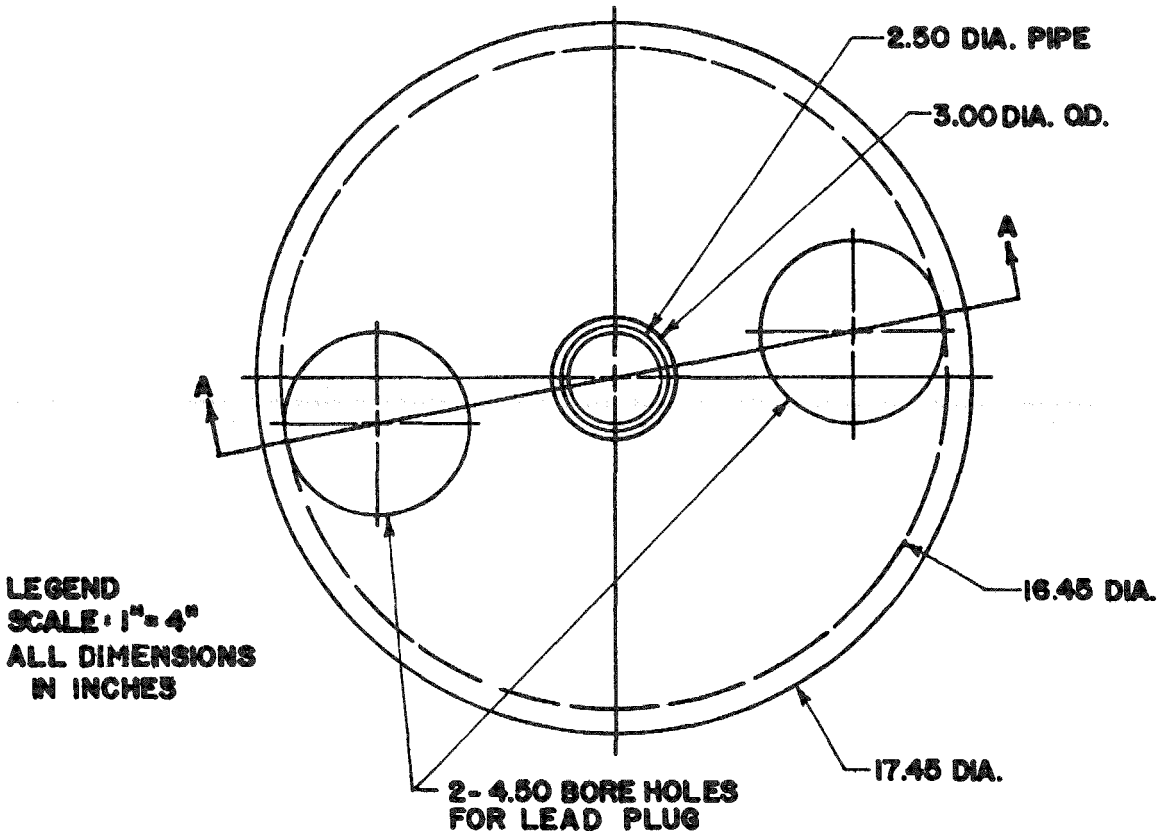

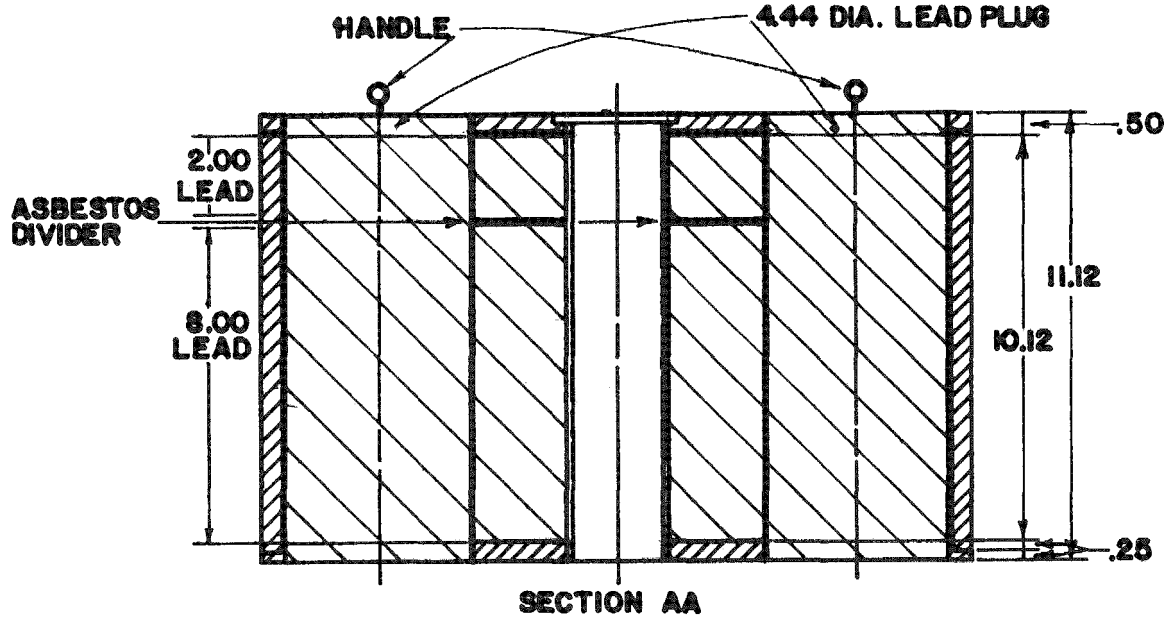

Figure 3-11 : Upper blanket can.

The bottom plate is the load bearing member. It is a full circle 1.727 m (68 in.) diameter, 102 mm (4 in.) thick, carbon steel plate bolted to a bearing ring located in a stepped recess at the top of the storage cask well. The top of the bearing ring is 102 mm (4 in.) below the floor to provide clearance at the top of the drive mechanism. This plate has a central 66.5 mm (2.62 in.) diameter hole for the source guide tube.

A central plate 17.3 mm (0.68 in.) thick and 443 mm (17.45 in.) diameter sits on top of the bottom plate and supports the inner and outer transformer cans. This plate is screwed to the base plate. The top surface has the locating holes for matching locating pins on the bottom of the outer transformer can. This plate has a central 91.9 mm (3.62 in.) diameter hole.

Two concentric annular, 180°-segmented rings of 130 mm (5.12 in.) thick plain steel plate are located under the radial blanket region. The inner, middle and outer diameters are respectively, 0.457 m (18 in.), 1.135 m (44.7 in.) and 1.473 m (58 in.). The split diameter is chosen as two-thirds of the blanket region width to allow for experiments using different length pins in the inner part of the blanket. They are split 180° to allow different experiments in each sector as well. The various plate thicknesses are chosen so that the fueled portions of the pins in the transformer regions and the natural U pins in the blanket align in a horizontal plane. The lower blanket grid plates rest on and are screwed to these plates. A 31.8 mm (1.25 in.) thick segmented plate nominally 1.463 m (58 in.) inner blanket, 1.778 m (70 in.) diameter outer diameter plain steel plate sets on the base plate to support the reflector cans.

The plates are painted with a red primer rust preventative. The bottom plate weighs approximately 1810 kg (4000 pounds) and is the heaviest item to be lifted by the service hoist. The inner and outer blanket 180° segments weight 210 kg (460 pounds) and 342 kg (753 pounds) respectively.

SOURCE STORAGE CASK

The source storage cask is a segmented concrete cylinder semipermanently located in the cask well in the floor of the experimental room. The vertical center line of the experimental assembly is common with the centerline of the storage cask. The source tube travels up and down along this axis between its storage position and its experimental position.

The cask is normally 2.42 m (95.5 in.) high by 1.52 m (60 in.) in diameter to provide approximately 0.76 m (30 in.) of ordinary concrete shielding in every direction from the source tube when it is in its stored position. A further 305 mm (12 in.) of reinforced concrete outside the cask forms the well for the cask and is considered permanent. A 9 mm (0.35 in.) layer of "Boraflex 50" containing 12 kg (26.41 lbs.) of B_4C is spread over the top of the cask as a thermal neutron shield.

The cask was cast in place in nine full height segments. The central segment is an octagon 462 mm (18.2 in.) across flats with a central 50 mm (2 in.) schedule 40 pipe. The eight peripheral segments are aligned with the octagon faces in a pinwheel arrangement so that no faces line up with the center hole. The segments were cast using greased plain sheet steel forms resting on a 25 mm (1 in.) bottom plate and in a cylindrical sheet steel can. The purpose of the segment is to facilitate disassembly at the end of the facility life. It is anticipated that jacks may have to be used to break the segments loose and full length rods with lugs have been cast into the concrete for this purpose. Each segment weighs about 1130 kg (2500 pounds).

The central pipe contains a polyethylene slug at its lower end. A machined steel cap at the top of the slug is screwed tightly to a rod that passes through the polyethylene and is welded to the cask bottom plate. This cap has a machined outer diameter that locates the bottom end of the source guide tube radially, a cross slot that provides a torque resistance to the source tube string, and a conical seat for the source tube to rest on the bottom of its travel. A curved stainless steel pipe 19.3 mm (0.76 in.) inside diameter is cast in one peripheral segment as a provision to locate a neutron detector in the storage cask. The tube ends at the source lower end (in the stored position). The upper end of the tube is aligned with an access tube cast into the floor of the experimental room (facing roughly in the direction of the instrumentation boxes on the room wall).

SOURCE DRIVE STRING AND DRIVE MECHANISM

A 316 stainless steel rod is attached to the top cap of the source tube by a mechanical bayonet connection. This rod provides the male half of the connection, full diameter shielding in the guide tube, and a physical stop to prevent source overtravel. The mechanical connection is a small steel cam sitting in a slot and held in by a spring. Pushing down on the rod and rotating 90° while

restraining the source tube will release the connection. A stop prevents over-rotation when making the connection. This extension rod is 198 mm (7.82 in.) long and 35.5 mm (1.40 in.) diameter. Both it and the outer surface of the source tube are "Magnaplated" (a propriety form of teflon coating) to reduce friction with the guide tube. Both the rod and the source tube upper end diameters prohibit their passing out through the 25.7 mm (1.01 in.) hole in the bushing at the top of the guide tube after assembly. The mechanical connection provides a degree of azimuthal freedom for source string alignment.

The upper end of the source extension rod is rigidly pinned to a 25.4 mm (1 in.) diameter 316 stainless steel drive rod that has a rack gear mounted in it. The tube and rack are long enough to accomodate the required vertical travel of the source string between its stored and experimental positions. A small 3 mm (0.12 in.) clearance exists at the top end between the experimental position and the physical stop.

In addition to the rack the drive rod has a full length slot in which a roller runs to prevent rotation. This keeps the rack and the pinion of the drive engaged. The drive rod runs through the brass cap at the top of the guide tube and is further supported by three rollers, at 90° intervals, on the drive support. When the source is fully raised the top end of the drive rod extends into a clearance hole in the bottom layer of the ceiling beams.

The source drive package is bolted to the top of the upper blanket and traps the bushing at the top of the guide tube. The package consists of a reversible 100 volt stepping motor, a gear train, a clutch, a brake, a pinion gear, position transducers, and a mounting frame. The clutch is electrically operated independently of the rest of the drive and performs the function of a remote quick-disconnect. It is a unique magnetic-particle type ("Soft-Step") and does not have clutch plates or springs as such. It is located between the pinion gear and the brake. When de-energized, it allows the source string to fall into the storage cask by gravity. The clutch supply voltage limits the force that can be applied by the drive to the source string. The brake is similar to construction to the clutch.

The source drive limits are set by microswitches mounted on the drive packages and activated by the drive rod. A ten-turn precision potention-meter is geared to the pinion gear and provides the primary indication of the source position.

The stepping function of the motor is not currently utilized. The time to raise the source into position is 0.7 minutes.

The drive motor, brake, and clutch supply currents are controlled from the control panel located outside the experimental room. A manual switch located inside the experimental room is provided in the clutch supply line. Figure 3-12 is a photograph showing the arrangement of converter regions, the source drive, the blanket grid plates, the outer reflector cans and a partical loading of the first blanket.

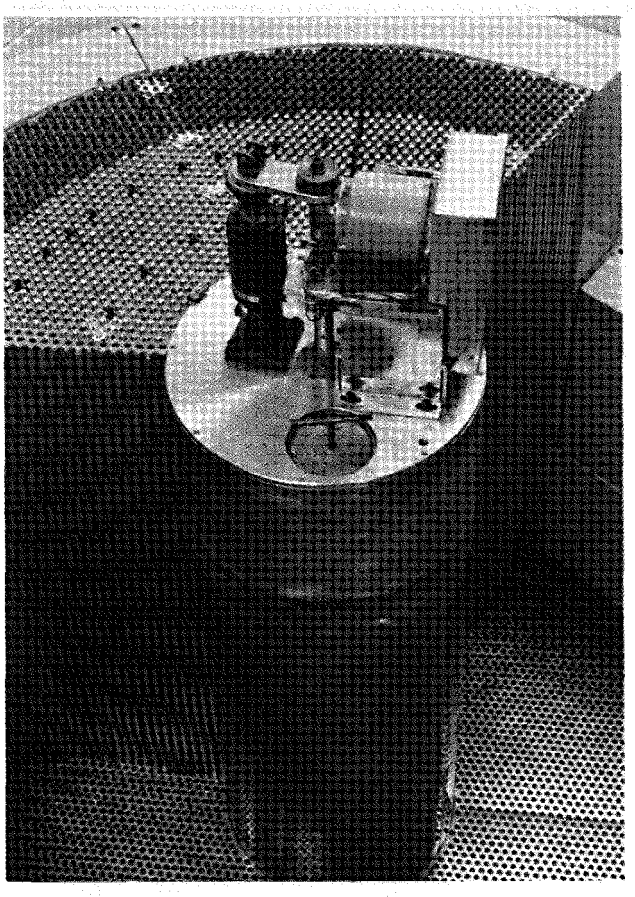

Figure 3-12 : The photograph of the FBBF facility shows the partially loaded initial blanket. The center of the picture shows the outer transformer can with the upper axial blanket can and source drive mechanism mounted on it. The lead plug visible in the upper blanket is removable to provide access to one of the two experimental locations in the outer transformer region. A number of yellow reflector cans that surround the facility and partially support the upper grid plate are also visable. The natural uranium oxide fuel rods are located in the top and bottom grid plate by pins. The different colored pins in the upper grid plate indicate whether the rods have stainless steel sleeves (gold), aluminum sleeves (blue) or are experimental rod positions (red).

FUEL PINS

The verious types of fuel pins available for use in the facility are shown in Fig. 3-13. Their dimensions are also listed in Table 3-1.

MATERIAL CONSTITUENTS

A list of the number densities for the various materials is given in Table 3-2.

Table 3-3 gives some of the more important transection areas for the main components.

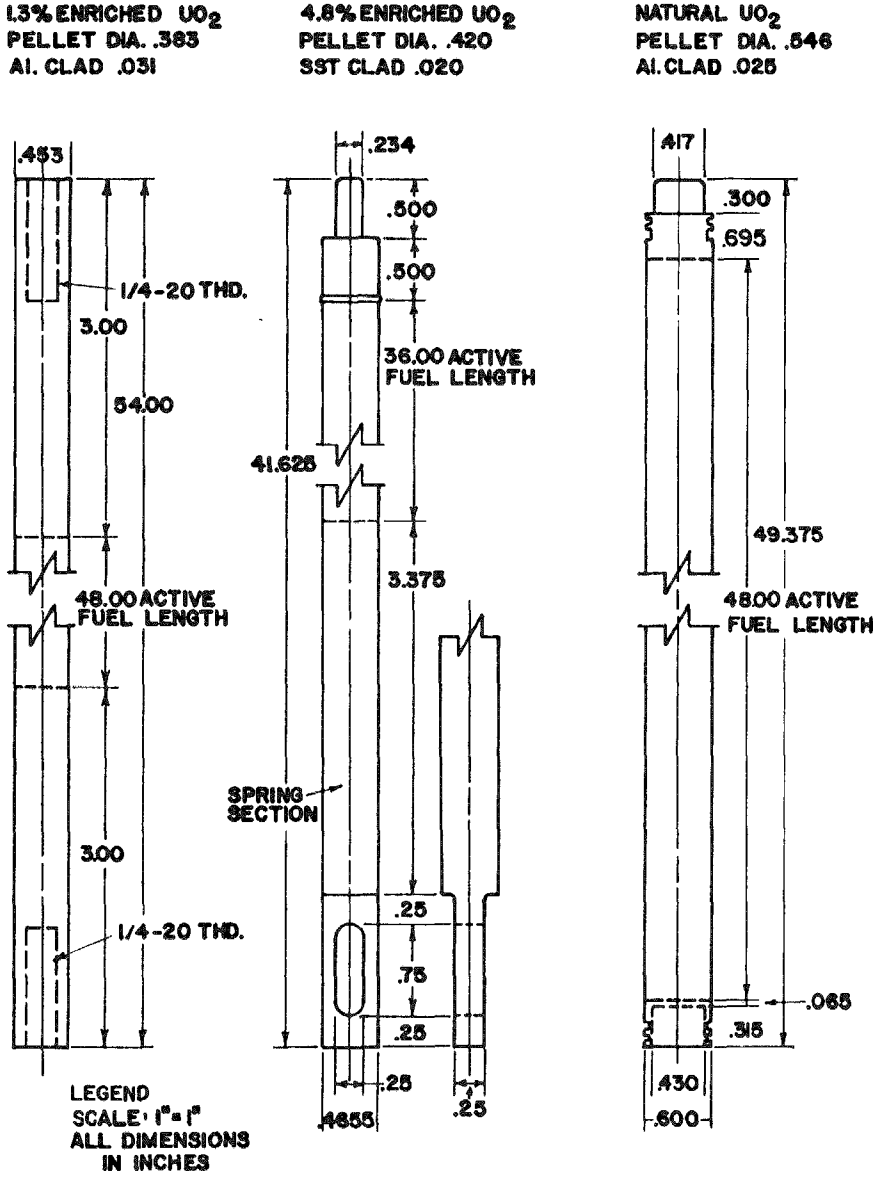

Figure 3-13: Fuel pin dimensions

Table 3-1
FUEL PIN DIMENSIONS

	Natural Uranium	1.3%	4.8%
Pellet Diameter	1.387 cm	0.973 cm	1.067 cm
Clad	Al	Al	348 St.St.
Clad OD	1.524 cm	1.151 cm	1.184 cm
Active Length	121.92	121.92 cm	91.44 cm
Overall Length	125.41 cm	137.16 cm	105.73 cm
Bottom Hardware	1.730 cm	7.620 cm	2.540 cm
Top Hardware	2.515 cm	7.620 cm	11.748 cm
Approx. Wt.	2.154 kg	1.361 kg	1.058 kg
Est. Clad ID	1.397 cm	.993 cm	1.082 cm
Clad Thicken	.064 cm	.079 cm	.051 cm
Clad Area	0.2914 cm^2	0.2652 cm^2	0.1808 cm^2
Gap Area	0.02219 cm^2	0.03135 cm^2	0.02574 cm^2
Fuel Area	1.5106 cm^2	0.7432 cm^2	0.8938 cm^2
Total	1.8239 cm^2	1.0398 cm^2	1.1003 cm^2
Clad VF	0.160	0.255	0.164
Gap VF	0.012	0.030	0.023
Fuel VF	0.828	0.715	0.812

Table 3-2

NUMBER DENSITIES FOR FBBF MATERIALS AND REGIONS (ATOMS/BARN-CM)

SS-304 (ρ = 7.75 gm/cc, Fe = 69% wt%, Mn = 2%, Cr = 19%, Ni = 10%)

Fe	0.0576672
Mn	0.0016992
Cr	0.0170555
Mi	0.0079500

SS-316 (ρ = 7.75 gm/cc, Fe = 67.5% wt%, Ni = 12%, Cr = 17%, Mn = 1%, Mo = 2.5%)

Fe	0.0564136
Ni	0.0095400
Cr	0.0152602
Mn	0.0008496
Mo	0.0012162

Carbon Steel (ρ = 7.75 gm/cc, Fe = 99.35% wt%, C = 0.2%, Mn = 0.45%)

Fe	0.0830325
C	0.00077720
Mn	0.00038231

Aluminum (ρ = 2.702 gm/cc)

Al	0.0603111

Nat. UO_2 Fuel (ρ = 10.97 gm/cc, 0.94TD, MW = 270.028 gm/gmole)

U-235	0.0001656
U-238	0.0228562
O	0.0460435

1.3% Enriched UO_2 Fuel (ρ = 10.97 gm/cc, 0.94TD, MW = 270.011 gm/gmole)

U-235	0.0002990
U-238	0.0227012
O	0.0460004

4.8% Enriched UO_2 Fuel (ρ = 10.97 gm/cc, 0.94 TD, MW = 269.905 gm/gmole)

U-235	0.0011044
U-238	0.0219048
O	0.0460184

B_4C, Inner Transformer (21.59 kg, ρ = 2.52 gm/cc, Packing Fraction 0.6124)

B-10	0.013323
B-11	0.053963
C	0.016821

B_4C, Outer Transformer (23.313 kg, ρ = 2.52 gm/cc, Packing Fraction 0.5358)

B-10	0.011655
B-11	0.047211
C	0.014717

Sodium, Outer Transformer (61.08 bm/pin, ρ = 0.97 gm/cc, Packing Fraction (0.9179)

Na	0.023324

Table 3-3

HORIZONTAL PLANE CROSS SECTION

	Material	Outer Radius (cm)	Area (cm^2)
Source			
CF Source	Cf	0.635	1.2668
(1) Space	Void	0.6477	0.05118
Source Holder	SS-316	1.270	3.7491
Space	Void	1.905	6.3338
Source Guide Tube	SS-304	2.540	8.8674
Space	Void	2.8575	5.3838
Inner Transformer			
Inner Wall	SS-304	3.4925	12.6677
Active Region	Mix	15.79956	745.9038
Outer Wall	SS-304	15.9893	18.9489
Space	Void	16.129	14.0961
Outer Transformer			
Inner Wall	SS-304	16.31874	19.3416
Active Region	Mix	21.97176	680.0196
Outer Wall	SS-304	22.1615	26.3072
Blanket			
Inner	Mix	56.810	8596.1641
Outer	Mix	73.660	6906.5386
Reflector			
Inner Wall	C1020	74.0103	162.5112
Salt Region	Salt	77.978	1894.5185
Wall	C1020	78.3283	172.0151
Steel Region	C1020	87.630	4849.6587
Outer Wall	C1020	88.900	704.3234
			24828.6665

OPERATING CONTROLS
(P. J. Fulford)

MOTOR DRIVE FOR SOURCE STRING

The motor is a single-speed reversible AC motor. It is controlled by a switch on the control panel. The circuit for the power supply to the motor is completed if all the following conditions are met:

1. --The door to the shielded area is closed and latched.
2. --The source drive is positioned below the source upper travel limit. This limit is several inches above the normal experimental "source up" position.
3. --The operating key is inserted into the "operating" switch.
4. --The conditions for the remote-disconnect latch are satisfied.
5. --Room ventilation system is activated.

Condition (2) is applicable only when the source string is being driven up. This is meant to limit the upward travel short of the mechanical stop.

To drive the source beyond the "source up" limit requires removing a mechanical limit stop from the drive and bypassing the limit switch.

SOLENOID-ACTIVÂTED REMOTE-DISCONNECT

The source assembly is attached to the source drive only if current is flowing to the remote solenoid. Otherwise, the weight of the source assembly causes the sources to fall freely into the storage cask.

The power circuit to the source remote-latch is completed if all the following conditions are met:

1. --The door to the shielded area is closed and latched.
2. --The operating key is inserted in the "operating" switch.
3. --The source assembly is positioned below the source upper travel limit position.
4. --None of several "source drop" switches located in or near the room are activated.
5. --The "source unlatch" switch is not activated on the control panel.

6. --AC power is available.

7. --Air ventilation system for the shielded room is activated.

ELECTRIC DOOR LATCH CONTROL

Access to the shielded area is controlled by the electric door latch. The latch is normally in the locked position. Supply of current allows the latch to unlock. For the current to flow all of the following conditions must be met:

1. --The source drive string must be at the "source down" limit.

2. --The source remote-disconnect mechanism must be in the "disconnect" position.

3. --The below-facility neutron monitor must indicate that the source is in the storage cask and the shielded-space radiation monitor must indicate a low level of room radiation.

4. --The operating key must be inserted in the "door open" switch, (thus the key cannot be in the "operating" switch).

5. --The "door open" pushbutton is activated.

6. --AC power is available.

A secondary security padlock is also on the door.

CONTROL PANEL

The control panel is located in the facility room with a direct view of the shielded room door and far enough away to require the presence of one person to operate the "door open" button for another person to open the door of the shielded facility. It is also positioned so as to be in a low radiation level area during source transferral operations.

RADIATION SHIELDING
(P. J. Fulford)

The shielding allows the following operations to be performed without undue hazard.

1. --Rearranging the experimental assembly with the source in the stored position.

2. --Entering the experiment room (B28C) with the source stored to retrieve experimental data.

3. --Work in the facility room (B28) with the source in the raised position.

4. --Hold classes and perform other usual operations in the surrounding portions of the Physics Building.

5. --Handle and store low level radiation sources such as foils and fuel pellets.

FBBF EXPERIMENTAL AREA

The shielded room (B28C) walls and ceiling form the biological shielding for the FBBF facility when the source is in the raised (experimental) position. In the lowered (stored) position the storage cask is the shield as the residual radiation of the experimental assembly will be minimal.

The walls are nominally 813 mm (32 in.) thick composed of 4 rows of concrete blocks filled with a high density morter. The blocks are hollow load-bearing blocks conforming to ASTM standards 1949 C90-59 grade A. The blocks in each row are offset by half their width and half their height from the next row neighbors to minimize streaming. The high density morter is Chemtree 1-20-26, a proprietory iron-ore type of material. Its density is a minimum 3.3 g/cm^{-3} (205 pounds/ cubic foot). The mixture of the concrete in the blocks and the high density morter in and around the blocks was treated during the design calculations as ordinary concrete.

The room ceiling is three layers of reinforced cast concrete beams weighing approximately 1 ton each. The bottom layer is set into the walls on a stepped ledge. The beams are installed offset from their vertical neighbors by a half-width to minimize streaming. The total thickness is 813 mm (32 in.). The bottom layer has a 127 mm (5 in.) hole at the location of the experimental assembly centerline to provide clearance for the source rod extension tube. A continuous 0.1 mm (4 mil.) plastic sheet is laid over this bottom layer and taped to the top of the walls to minimize air-in leakage to the room through the ceiling. The beams can support a further loading of approximately 300 kg/m^2 (60 pounds/sq.ft.) if this should be required.

An interior wall of the same composition and thickness as the exterior wall blocks direct leakage out of the doorway. To prevent secondary scattering two further concrete blocks (solid) columns are installed (dry) in the maze passage giving a tortuous path for scattered radiation.

FUEL HANDLING SHIELDED HOOD

A ventilated box with 25.4 mm (1 in.) steel walls is provided for handling objects where there exists a possibility of dust dispersal such as opening a fuel pin to insert foils. The interior cross section of the box is 305 mm x 305 mm (12 in. by 12 in.) and the interior length is 3.05 m (10 ft.). Hatches are provided along the top of the box and at each end for access. Air is drawn from the back of the box through a long slot and passed through a HEPA filter before being exhausted to the atmosphere. Air enters the box through the hatch openings which are sized and regulated to maintain a nominal 0.5 m/s^{-1} (100 fpm) face velocity.

A piece of 25 mm x 25 mm (1 in. x 1 in.) angle iron is welded along the bottom of the box to provide a holding groove for fuel pins. Lights are installed at each end for visibility. The hatch covers can be clamped closed against rubber gaskets when not open. The box and its supports are sufficiently strong to allow lead blocks to be installed in it for further shielding if this should be required.

EXPERIMENTAL EQUIPMENT
(F. M. Clikeman and R. H. Johnson)

Several major pieces of experimental equipment have been acquired for the FBBF laboratory. These include a Ge(Li) detector, a computerized data acquisition system, and a thermoluminescent dosimeter (TLD) reader. Experiments for which these equipment will be used are described in Section VI.

The Ge(Li) detector is a Canberra model 7229 with a resolution of 2 keV (FWHM) and relative efficiency of 13% at the 1332 keV photopeak of ^{60}Co. The detector (together with its preamplifier and cryostat) is provided with a shield against background radiation. The shield assembly allows for 8 inches of lead above the detector and around the side of the detector; 1.5 inches of steel shielding is located below the detector. (The liquid nitrogen in the cryostat also provides some shielding below the detector.)

A Canberra Scorpio 3000 system provides the FBBF laboratory with data acquisition, graphics display, and data analysis capabilities. This system is based on a PDP-11/04 minicomputer with 28K words of core memory. A separate 16K words of core memory is present for storage of pulse height spectra during data acquisition. The system includes two analog-to-digital converters which can be config-

ured for two-parameter data acquisition. The system also includes a dual floppy disk drive for program and data storage and a DEC writer for use as an input and hardcopy output device.

The Scorpio 3000 software operates under the Digital Equipment Corporation RT-11 operating system; either single job or foreground/background modes of operation may be selected. The RT/SCORPIO software package includes all routines used during data acquisition and provides standard functions such as peak area and centroid computation for efficiency and energy calibration. The SCORPIO/SPECTRAN software package provides the necessary routines for a quantitative isotopic analysis of gamma-ray spectra measured with a Ge(Li) detector; similar software is available for analysis of spectra measured with a NaI(Tl) detector.

Gamma heating measurements are being made using thermoluminescent (TLD) dosimetry. Dosimeters selected for the initial measurements are CaF_2:Dy crystals, 1/8" x 1/8" x 0.035". Calcium flouride was selected as the TLD dosimeter after considering factors such as the atomic number of the dosimeters, fading and sensitivity.

Readout of the dosimeters is accomplished with a Harshaw model 2000-A TL detector and model 2000-B automatic integrating picoammeter. This system provides linear heating rates for the analysis as well as, thermal isolation and thermoelectric cooling of the phototube. The analyzer system, with its wide range of heating rates, high temperature range and sensitivity allows a wide range of TLD materials to be analyzed. A builtin Radium activated NaI(Tl) light source and provisions for flowing dry gas through the sampling chamber permit a high degree of reproducibility in the analyzer system. The system also permits all of the common geometries of TLD's, including powders, to be analyzed. Both X-Y recorders and strip chart recorders are available for readout of the picoammeter as well as the digital current integrator.

In addition to the TLD analyzer, a furance for both pre- and post-annealing of the dosimeters is available. The furnace is capable of temperatures in excess of 300° C, allowing it to be used with all of the more common TLD dosimeters. A rotating exposure holder has been built which will allow all of the dosimeters to be exposed to a uniform exposure and then to be grouped on the basis of uniformity of response. Calibrated gamma sources are also available to determine the absolute calibration of the TLD's and analyzer system.

4

NEUTRON AND GAMMA-RAY FLUX CALCULATIONS

NEUTRON ENERGY SPECTRA COMPARISON
(R. C. Borg, J. H. Paczolt and D. M. Waite)

One of the basic objectives of the FBBF is to generate spectra in the blanket which are similar to spectra found in a large fast breeder reactor blanket. The conceptual design study (16) indicated a good match between spectra generated by the FBBF and a typical 1000 MWe fast breeder reactor. A number of modifications have been implemented into the original design. Therefore, it is desirable to compare spectra generated from the final design of the FBBF with typical fast breeder reactor blanket spectra.

The physical and geometrical characteristics of the FBBF and a modified 1000 MWe Clinch River Breeder Reactor [CRBR (17)] were mocked-up with the one-dimensional computer code LAZARUS (18). The desired neutron flux calculations were preformed to determine the spectrum. In these comparisons, the blanket of the modified CRBR was identical to the initial loading of the FBBF.

The normalized spectrum from each calculation for the blanket interface, middle of the inner blanket, inner and outer blanket interface and middle of the outer blanket are plotted in Figs. 4-1 to 4-3. The midpoint of each group is connected for better comparison. For all illustrated space points the spectrum calculated for the FBBF is very representative of the spectrum calculated for the modified CRBR. Thus, one of the basic objectives of the FBBF to generate spectra characteristics of large fast breeder reactors has been accomplished.

SOURCE AXIAL DISTRIBUTION
(R.C. Borg, M. P. Sohn, J. H. Pazolt and D. M. Waite)

Previously, axial and radial reaction rate traverses were calculated from fluxes generated by a line source with an axial chopped cosine strength distribution (19). These initial investigations showed that sample blanket region axial reaction rate traverses fit a chopped cosine extremely well. The ^{252}Cf source in the FBBF is not a line source but actually consists of four point sources of different

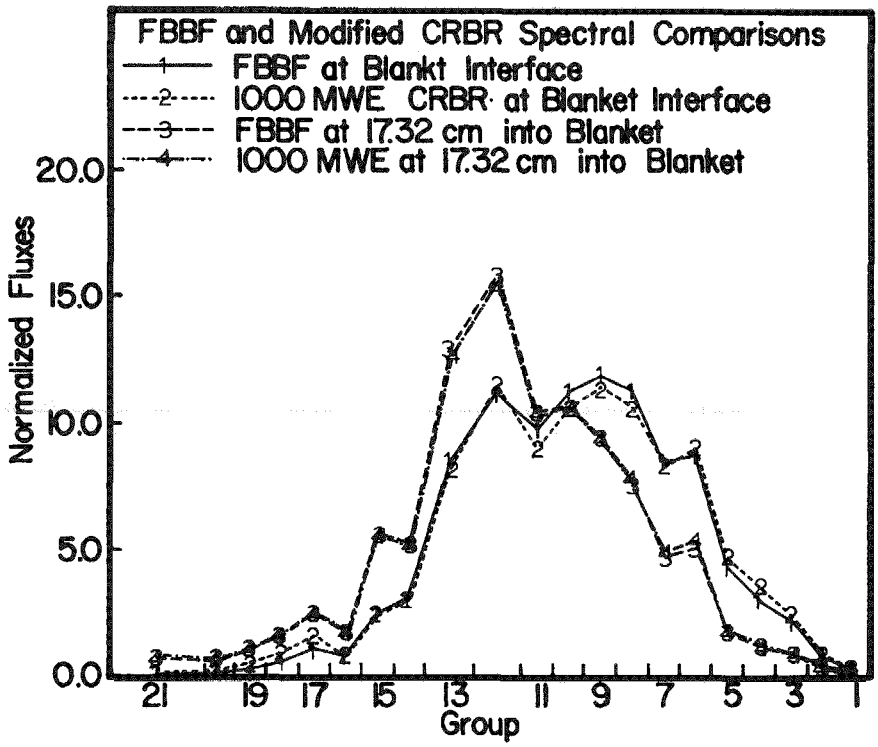

Figure 4-1: FBBF and modified CRBR spectrum at the inner blanket interface and at the midplane of the inner blanket.

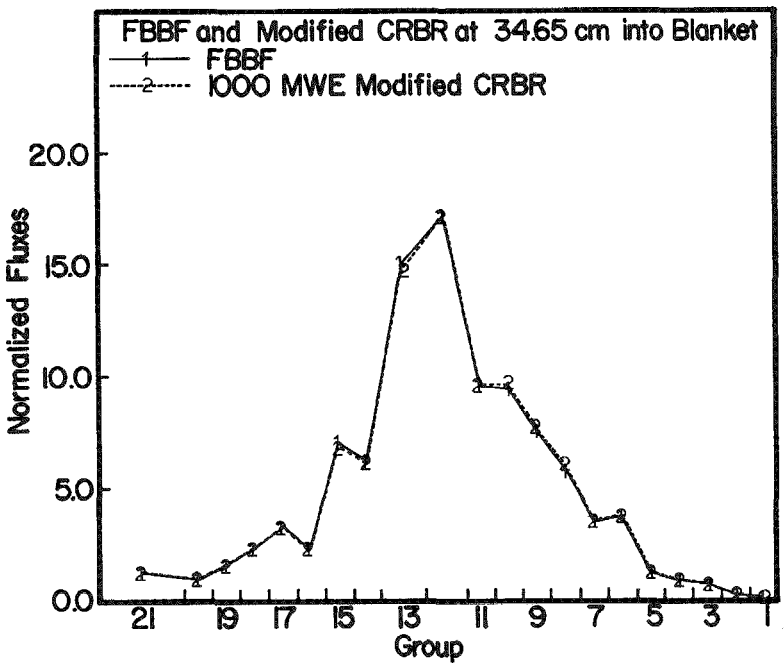

Figure 4-2: FBBF and modified CRBR spectrum at the inner and outer blanket interface.

strength. Their positions in the source rods were predetermined to give a chopped cosine flux distribution in the blanket region, with the maximum value at the axial mid-plane. In this subsection, comparison of the total flux and sample reaction rates generated from both the line source and discrete point sources are investigated.

The calculational procedure and two-dimensional model needed for the source distribution investigations are the same as those used for the sample reaction rate calculations presented in Ref. 19. The same 21-group constant set is also used. The inherent problem of the 21-group library lower energy group structure will not hamper the interpretation of results since the contributions of the lowest energy group are neglected as was suggested (19).

The axial shape of the flux and reaction rates are directly influenced by the strength and position of the four discrete sources. In Figs. 4-4 and 4-5, the axial shape of the total flux, at the converter blanket and blanket midplane, is illustrated. The solid line represents the flux generated from a line source. The smallest dashed lines indicate the flux generated from the calculation with four discrete sources. The maximum value of the total flux, generated by the

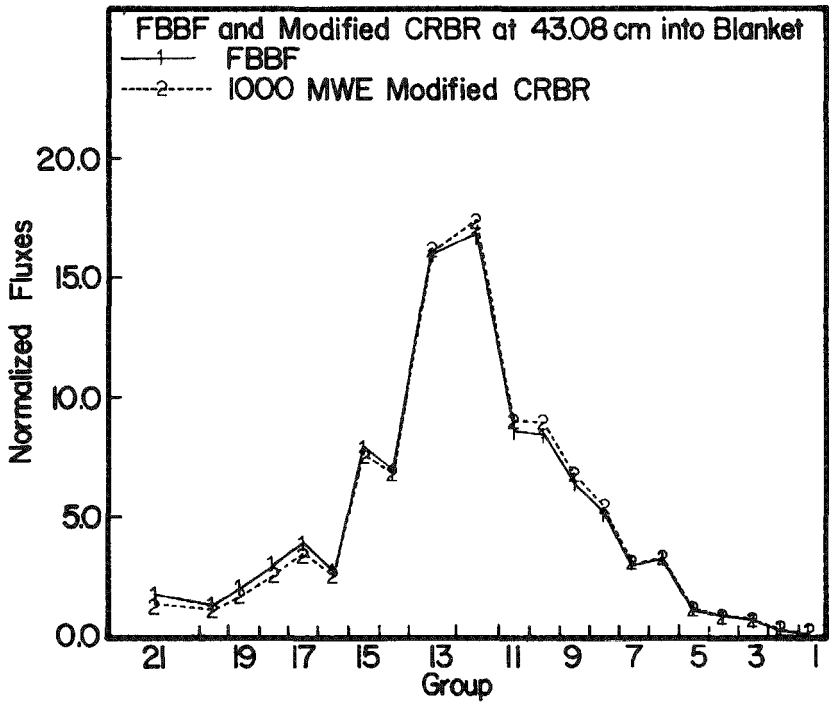

Figure 4-3: FBBF and modified CRBR spectrum at the midplane of the outer blanket.

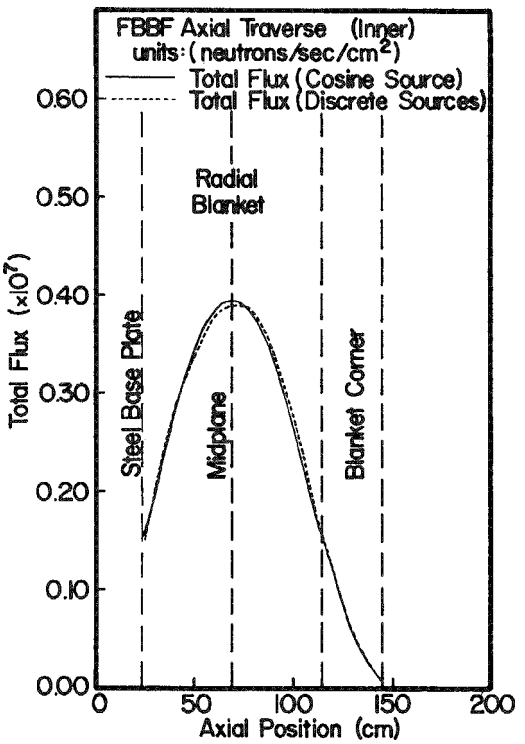

Figure 4-4: Axial flux shape at the converter-blanket interface.

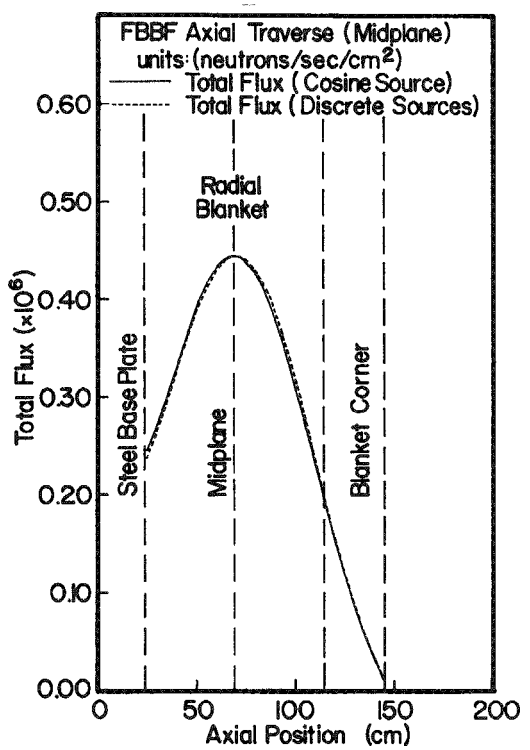

Figure 4-5: Axial flux shape at the blanket midplane.

discrete source, at the converter blanket interface is shifted slightly above the center line, (compare Fig. 4-5). Further out into the blanket the maximum value of the total flux generated by the discrete sources is much closer to the axial midplane. As indicated in both figures, the discrete point sources generate a flux shape which is very close to the flux shape associated with cosine shaped line source.

GAMMA-RAY ENERGY DEPOSITION RATES
(R. H. Johnson, J. H. Paczolt)

Gamma-ray energy deposition measurements using thermoluminescent dosimetry (TLD) will be part of the experimental program for the FBBF. One-dimensional discrete ordinates calculations have been made of the gamma-ray heating rates to aid in planning the TLD measurements. Gamma-rays are produced throughout the FBBF by radiative capture, fission, and inelastic scattering. Gamma-rays are also emitted by the ^{252}Cf spontaneous fission source. Because the gamma-ray flux is strongly dependent on the neutron flux, a coupled neutron and gamma-ray transport calculation was performed for the preanalysis of the gamma-ray heating rates.

ANISN-W (20), a one-dimensional discrete ordinates code including treatment of anisotropic scattering, was obtained from the Radiation Shielding Information Center (RSIC) of Oak Ridge National Laboratory. The DLC-37/EPR cross section set (21,22) based on ENDF/B-IV data was also obtained from RSIC. DLC-37/EPR contains coupled (100-neutron, 21-gamma-ray groups) P_8 cross sections as well as neutron and gamma-ray kerma (kinetic energy released in material) factors for many important elements.

The large number of neutron groups in DLC-37/EPR necessitated group collapsing in order to perform the preanalysis calculations on the Purdue dual CDC-6500 system. ANISN-W was used for the group collapsing to 23 neutron groups. Slight modifications of ANISN-W were found necessary for the correct collapsing of a coupled cross section set (23).

An S_4,P_3 calculation was performed for the preanalysis using a one-dimensional model of the FBBF (24) and a transverse leakage correction. The TLD measurements will give, to a first approximation, the gamma-ray energy deposition rate in the material surrounding the dosimeter. Several different materials are of interest. Preanalysis calculations of the gamma-ray energy deposition rates in type 316 stainless steel, lead, and UO_2 are shown in Figs. 4-6. 4-7 and 4-8.

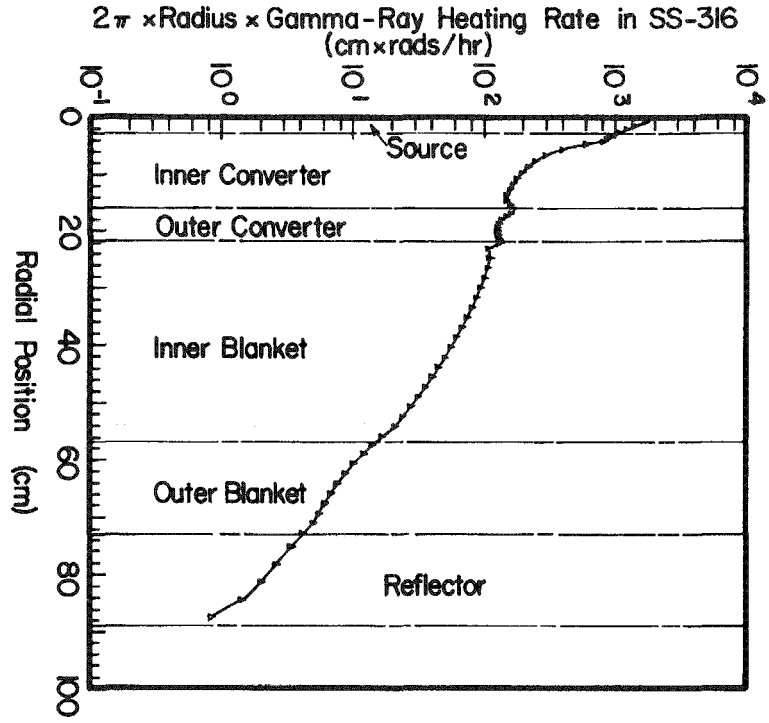

Figure 4-6: S_4,P_3 ANISN-W calculation of gamma-ray energy deposition rate in type 316 stainless steel for blanket height of 159.52 cm.

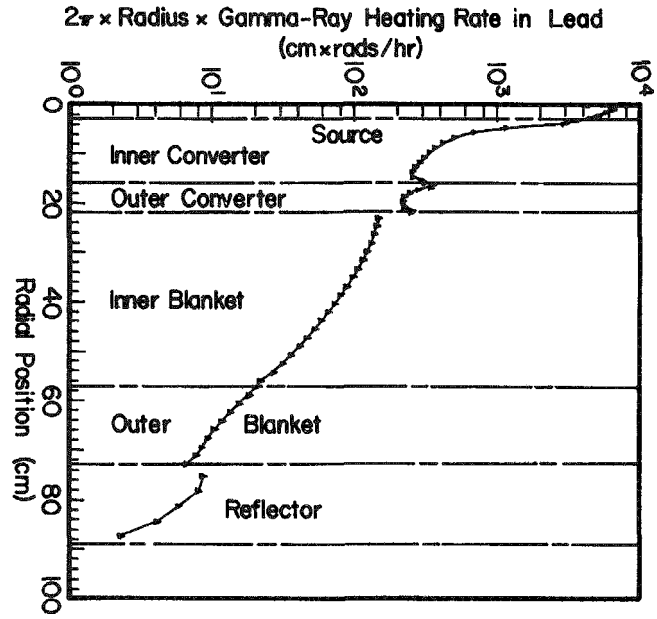

Figure 4-7: S_4,P_3 ANISN-W calculation energy deposition rate in lead for blanket height of 159.52 cm.

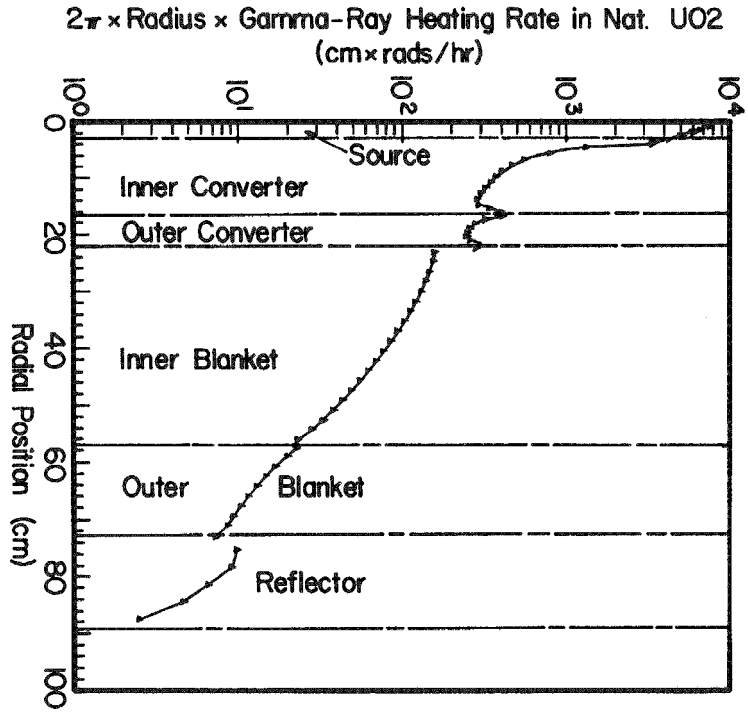

Figure 4-8: S_4,P_3 ANISN-W calculation of gamma-ray energy deposition rate in natural UO_2 for blanket height of 159.52 cm.

[Heating rates in uranium were obtained by extrapolation (25).] The calculations are normalized to represent a radial traverse along the axial midplane of the blanket. These results can be used in planning the TLD measurements.

A different cross section set will be used for the final calculations because DLC-37/EPR has two shortcomings. First, a thermal temperature of 800°K was used in producing DLC-37/EPR; as a result, cross sections in the resonance region are higher than they should be for room temperature. Second, delayed gamma rays from fission are not included in DLC-37/EPR. Further calculations will be made using ANISN-W and a new cross section set. It will also be necessary to use a two-dimensional transport code for the final calculations, especially if heating rates near the top and bottom of the radial blanket (or actually in the axial blanket) are to be calculated.

5

SAFETY INVESTIGATION
(R.C. Borg)

The FBBF is a fast neutron subcritical facility. Thus, for normal operation, there is an insignificant number of low energy and thermal neutrons due to the absence of moderating materials. Safety of the FBBF is primarily concerned with the hypothetical flooding accident, which would inject water, as a moderator, into the system causing moderation of neutrons which could decrease the degree of subcriticality. Since the FBBF is located below ground level, flooding is possible if large amounts of water were necessary to extinguish a fire. The FBBF is designed such that it could not accidently become critical or come close to a critical state for any flooded condition.

In this section the results of the safety investigations of the hypothetical flooding accident reported in Refs. 24 to 30 are summarized. Vibrating B_4C into the converters was not initially contemplated. Therefore, the impact of boron in dry and flooded converters were not considered in some of the early safety studies. Initially one-dimensional FOG code calculations were used to evaluate k_{eff} for various dry-flooded conditions, but for a presumed initial loading configuration without boron in the converters (24). Later, two models for the geometrical mockup of the FBBF, one with and one without explicit treatment of B_4C transition regions in the converters were used as input to the two-dimensional 2DB code (32). The value of k_{eff} of the hypothetical accident for a range of loading conditions, which included pitch variations and different types of secondary cladding, were determined. The inherent safety feature of the FBBF with both the inner and outer converters dry or flooded were evaluated. The results of these invesitgations are discussed and summarized here.

The composition of each region of the FBBF was determined from the initial loading configuration. The initial loading of the radial blanket has the inner two-thirds of the natural uranium fuel pins surrounded with stainless steel secondary cladding and the outer rows are double clad with aluminum or stainless steel double clad blanket rather than the initial loading configuration. Two blanket pitches were chosen to illustrate the effect of pitch variation under various dry-flooded

conditions. The initial blanket loading pitch, 17.1 mm (0.673 in.) and the pitch of the maximum reactive configuration, 22.9 mm (0.900 in.), i.e., the configuration which results in the maximum k_{eff} in the all Al blanket, are the basis for some of the presented material.

The pitch in the inner converter was slightly increased from the original design value of 11.9 mm (0.468 in.) to 12.0 mm (0.474 in.). The amounts of natural B_4C vibrated into the inner and outer converters are 21.59 kg and 23.313 kg, respectively. It occupies 61.24 percent of the possible voided volume of the inner converter and 53.58 percent of the outer converter. These amounts of B_4C are very close to the originally assumed value of 60 percent. The source region was considered to be flooded with and without the source plug in place in order to compare results with the original investigations (24). Because the reflectors are also welded shut, they were treated as dry regions for most of the cases.

The unit cell description for the input to the HAMMER code (33), which generated group constants in each region, is reported in Ref. 30. The material number densities and explicit dimensions used in the models are also given in Ref. 30.

RESULTS AND DISCUSSION

The effective multiplication factors, calculated with the model which explicitly treats the B_4C transition regions, for various conditions are presented in three tables. Table5-1 gives values of k_{eff} for a pitch of 17.1 mm (0.673 in.), Table 5-3 for a pitch of 22.9 mm (0.900 in.) with Al as secondary cladding. The k-infinite values which are helpful in understanding the results are given in Table 5-4 for the converters and blankets.

Several important features about the safety behavior of the FBBF are discussed in the following.

(1) Boron effect in the inner and outer converters:
The presence of B_4C in the converters stabilizes the value of k_{eff} for a given blanket pitch with the converters treated as dry or flooded (compare the first four cases in Tables 5-1, 5-2 and 5-3. Every region in the FBBF has some contribution to the value of k_{eff}, but the degree of its influence depends on the magnitude of k_{∞}, and the size and the location of the region. All of the fuel of the FBBF is loaded in the converters and blanket, therefore, these regions

have the dominant impact on the value of k_{eff}. The values of k_{∞} as shown in Table 5-4, for flooded converters with boron are only slightly smaller than the k_{∞} values of the dry converters with boron (compare Cases No. 2 and 4; 6 and 8 in Table 5-4. This trend is due to the compensation between the increased absorption of B_4C and fission of U-235 as the neutron spectrum becomes softer for the flooded case. Therefore, if boron is in the dry or flooded converters, there is not much difference in the value of k_{eff} since the k_{∞} value of the converters is not significantly different for the two conditions.

For the boron free converters k_{eff} greatly increases when comparing dry and flooded cases for the same blanket pitch (compare cases 5 to 8 in Tables 5-1. and 5-2. This increase is more pronounced for the initial loading pitch than the larger pitch of 22.9 mm (0.900 in.). The values of k_{∞} are much smaller for the dry converters without boron than the flooded converters without boron (compare cases No. 1 and 3; 5 and 7 of Table 5-4. All of these values of k_{∞} are sufficiently larger than k_{∞} of the blanket with the initial loading pitch (compare Case 9). For the SS double clad blanket with a pitch of 22.9 mm (0.900 in.) the value of k_{∞} is larger than the k_{∞} of the dry OC without boron. The blanket has proportionately a greater contribution for the case with a pitch of 22.9 mm (0.900 in.) when compared to the blanket with a pitch of 17.1 mm (0.673 in.) due to the increased value of k_{∞}. Thus, one would expect k_{eff} to increase when comparing cases with dry versus flooded converters without boron. Also, the increase should be more pronounced for the case with the blanket initial loading pitch since the converters contribute more. This trend is indicated in Tables 5-1 and 5-2.

(2) The impact of wet reflectors:
Case 9 in Table 5-2 considered all regions of the FBBF flooded. As illustrated in the table, the value of k_{eff} is identical to that of case 8 which has a dry reflector. Thus, the impact of a dry versus wet reflectors is minimal.

(3) The impact of water in the source region:
For the cases with boron in the converters, k_{eff} changes very little even if the stainless steel plug in the source region is replaced with water for both SS and Al double clad blankets (compare the first four cases in Tables 5-1, 5-2 and 5-3),

Water in the source region can soften the neutron spectrum in the adjacent regions, and thus influence these regions. The boron in the converters has a stabilizing

effect as stated above. The importance of these effects i.e., boron stabilization or water in the source, depends on the values of k_∞ in the converters and the blanket. Since the values of k_∞ for the converters with boron are not much larger than those of blankets and in some cases even smaller (compare Cases No. 2, 4, 6, 8, 9, 10 and 11 of Table 5-4), the boron stabilizing effect is dominant and water in the source does not effect the system. Therefore, the replacement of the SS source region with water has negligible effect on the values of k_{eff} for the cases with boron in the converters.

For the boron free converters, k_{eff} has a negligible change in the dry converter cases, but there is a slight increase in the flooded cases when the stainless steel plug in the source region is replaced with water (compare Cases 5 and 7; 6 and 9 in Tables 5-1 and 5-2). Since no boron stabilizing effect exists, the values of k_{eff} are influenced by the addition of water in the source region. The values of k_∞ for the flooded converters without boron are much larger than those of SS double clad blankets (compare Cases No. 3, 7, 9 and 10 of Table 5-4). Therefore, the source region with water has a larger influence for the flooded cases without boron.

(4) The effect of pitch variation:
The values of k_{eff} increases as the pitch of the blanket increases until there is a trade off between moderation and production. Results are presented in Ref. 30. The increase in k_{eff} is due mainly to the increase in k_∞ from 0.4705 for the pitch 17.1 mm (0.673 in.) to 0.6831 for the pitch 22.9 mm (0.900 in.) for the SS double clad blanket (compare Cases No. 9 and 10 of Table 5-4). Any increase in the pitch beyond the reactivity maximum will cause the value of k_{eff} to decrease since the blanket becomes over moderated.

(5) SS double clad vs Al double clad:
If the Al double clad fuel pins are used instead of SS double clad fuel pins, k_{eff} increases for the same pitch. Comparing the last two cases in Table 5-4, k_∞ increases from 0.6831 to 0.8583, for the defined secondary cladding change in the blanket, which inturn will cause k_{eff} to increase.

(6) The comparison of models:
The values of k_{eff} calculated by the three models mentioned in the introduction are given in Table 5-5 for the boron-free cases with the blanket pitch of 17.1 mm (0.673 in.). Models 1 and 2 are used with the two-dimensional 2DB calculation

with and without the transition regions treated, respectively. Model 3 is the basis of the one-deimsnional FOG calculation of Ref. 24.

The values of k_{eff} obtained from Models 2 and 3 agree very well, but are a little higher than those evaluated from Model 1 for the dry cases, while the converse is true for the flooded case. The increasing trend in k_{eff} when comparing dry and flooded cases is the same for the three models. The improved two-dimensional model, Model 1, which is the basis for the most resent investigations, should give more reliable results.

CONCLUSIONS

The use of improved methods and models in the safety investigation of a hypothetical flooding accident has led to several important conclusions which are summarized here.

(1) Boron in the converters has a stabilizing effect irrespective of whether they are treated as dry or flooded cases, i.e., for a hypothetical flooding accident k_{eff} stays fairly constant for dry or flooded converters when B_4C is present. If there is no B_4C in the converters, k_{eff} would greatly increase when comparing the dry converter cases to flooded converter cases. However, boron in the converters still can not bring the values of k_{eff} below 0.75 for Al double clad blanket with the most reactive pitch of 22.9 mm (0.900 in.) (compare Table 5-3).

(2) Explicit treatment of dry vs flooded reflectors has little impact on the value of k_{eff}.

(3) The replacement of the stainless steel in the source region with water has only negligible effect on the FBBF except for the case of the flooded converters without boron.

(4) Increasing the pitch from the initial value causes k_{eff} to initially increase until there is a trade off between moderation and production. Then the value of k_{eff} decreases as the pitch is continuously increased from the pitch of the maximum reactivity.

(5) The change from SS double clad blanket to Al double clad blanket results in an increase in k_{eff} (27).

(6) The results from the three models are in very good agreement and the trends for different dry-flooded conditions are the same.

Table 5-1

VALUES OF k_{eff} FOR VARIOUS DRY-FLOODED CONDITIONS
FOR SS DOUBLE CLAD BLANKET WITH A PITCH OF 17.1 mm (0.673 in.)

Case No.	Source	IC	OC	B_4C	Blanket	Reflector	k_{eff}
1	SS	D	D	Y	F	D	0.41027
2	SS	F	F	Y	F	D	0.40507
3	F	D	D	Y	F	D	0.41259
4	F	F	F	Y	F	D	0.40693
5	SS	D	D	N	F	D	0.46846
6	SS	F	F	N	F	D	0.72101
7	F	D	D	N	F	D	0.46953
8	F	F	F	N	F	D	0.76546

The symbols used in the table:
IC - Inner Converter
OC - Outer Converter
SS - Stainless Steel plug
D - Dry
F - Flooded
Y - B4C in converters
N - No B4C in converters

Table 5-2

VALUES OF k_{eff} FOR VARIOUS DRY-FLOODED CONDITIONS
FOR SS DOUBLE CLAD BLANKET WITH A PITCH OF 22.9 mm (0.900 in.)

Case No.	Source	IC	OC	B_4C	Blanket	Reflector	k_{eff}
1	SS	D	D	Y	F	D	0.61864
2	SS	F	F	Y	F	D	0.61668
3	F	D	D	Y	F	D	0.61858
4	F	F	F	Y	F	D	0.61669
5	SS	D	D	N	F	D	0.64959
6	SS	F	F	N	F	D	0.75855
7	F	D	D	N	F	D	0.64974
8	F	F	F	N	F	D	0.79170
9	F	F	F	N	F	F	0.79171

The symbols used here are the same as Table 5-1.

Table 5-3

VALUES OF k_{eff} FOR VARIOUS DRY-FLOODED CONDITIONS
FOR AL DOUBLE CLAD BLANKET WITH A PITCH OF 22.9 mm (0.900 in.)

Case No.	Source	IC	OC	B_4C	Blanket	Reflector	k_{eff}
1	SS	D	D	Y	F	D	0.77529
2	SS	F	F	Y	F	D	0.77168
3	F	D	D	Y	F	D	0.77518
4	F	F	F	Y	F	D	0.77167

Table 5-4

k-infinity FOR INNER CONVERTER, OUTER CONVERTER
AND BLANKET UNDER VARIOUS CONDITIONS

Case	Region	Conditions		k_∞
1	IC	dry, no B_4C		0.7905
2	IC	dry, with B_4C		0.5589
3	IC	flooded, no B_4C		0.9403
4	IC	flooded, with B_4C		0.5218
5	OC	dry, no B_4C		0.6576
6	OC	dry, with B_4C		0.4539
7	OC	flooded, no B_4C		0.7755
8	OC	flooded, with B_4C		0.4493
9	Blanket	flooded, 17.1 mm	SS double clad	0.4705
10	Blanket	flooded, 22.9 mm	SS double clad	0.6831
11	Blanket	flooded, 22.9 mm	Al double clad	0.8583

IC - Inner Converter
OC - Outer Converter

Table 5-5

VALUES OF k_{eff} CALCULATED BY VARIOUS MODELS
FOR 17.1 mm (0.673 in.) SS DOUBLE CLAD BLANKET UNDER
VARIOUS CONDITIONS WITHOUT BORON IN CONVERTERS

Case No.	Model	Source	IC	OC	Blanket	Reflector	k_{eff}
1	1	SS	D	D	F	D	0.46846
2	1	SS	F	F	F	D	0.72101
3	1	F	D	D	F	D	0.46953
4	1	F	F	F	F	D	0.76546
5	2	SS	D	D	F	D	0.49537
6	2	SS	F	F	F	D	0.64788
7	2	F	D	D	F	D	0.56906
8	2	F	F	F	F	D	0.71030
9	3	SS	D	D	F	F	0.4884
10	3	SS	F	F	F	F	0.6486
11	3	F	F	F	F	F	0.7180

The Model No.
1 - model with explicit treatment of transition regions.
2 - model without explicit treatment on transition regions.
3 - one dimensional FOG calculation.

6

EXPERIMENTAL MEASUREMENTS TO VERIFY CRITICALITY AND SHIELDING CALCULATIONS
(F.M. Clikeman)

Permission from the Nuclear Regulatory Commission to operate the FBBF facility was granted to Purdue University as part of their special nuclear material license SNM-142. (Dec. 17, 1976). Several special conditions covering the operation of the facility were added to the license. These conditions included verifying the shielding calculations and checking the multiplication of the facility under normal conditions. Significant differences between measured and calculated values were to be reported to the NRC. The following two sections summarize the results of the measurements.

MEASUREMENT OF THE k_{eff} OF THE FAST BREEDER BLANKET FACILITY
(F.M. Clikeman)

Subject to the conditions of the license covering the operation of the FBBF facility, measurements of the k_{eff} were completed. A PuBe neutron source together with ^{3}He neutron detector were used to make source multiplication measurements of the FBBF loaded with its first blanket of natural uranium rods. The neutron detector was placed in a paraffin cylinder to increase the sensitivity to epithermal and fast neutrons, giving an almost uniform sensitivity over a wide neutron energy range. Counting rates for the neutron source alone were established outside the shielded FBBF room by carefully mocking-up the source-detector spacing together with steel to represent the steel in the FBBF reflector cans. Concrete blocks were placed behind the source and detector to correct for the effects of the shielding walls of the FBBF facility. The source and detector where then positioned diagonally opposite each other in the shielded room and centered on the FBBF facility. The measured source multiplication is 1.673 ± 0.011 which yields a k_{eff} equal to 0.40 ± 0.01. The above reported errors are due to counting statistics alone. The estimated overall error in k_{eff} is ± 0.04. Two calculated values of k_{eff} were included in the license application. The calculated values are for the transformer regions without the boron carbide filling the interstitial regions. However, boron carbide is not expected to affect the dry (unflooded) k_{eff}. The reported calculated values were 0.400 ± 0.015 and 0.416. Agreement between the measured and calculated values is excellent. Both the measured and

calculated values are below the 0.45 value stated in the condition 15 of the SNM-142 license governing the operation of the FBBF facility.

COMPARISON OF SHIELDING MEASUREMENTS AND CALCULATIONS FOR THE FBBF
(R.H. Johnson)

Condition 14 of the license for the FBBF states "...the licensee shall, within thirty days after start of operation of the Fast Breeder Blanket Facility (FBBF), measure radiation levels outside of the facility to confirm the calculations summarized in Section E of the August 10, 1976, application, and take appropriate corrective action, if required." A short initial operation of the FBBF was carried out on April 8, 1978 with preliminary shielding measurements performed at that time. After that initial operation, planned additional shielding was added to improve the maze for the doorway to room B28C. Later shielding measurements have been made, primarily during the period May 5-8, 1978.

The gamma-ray dose rate measurements were made using a Ludlum NaI(Tl) counter and scaler. Additional gamma-ray dose rate measurements for the preparation room, lecture room and seating area using TLD dosimeters are also being made. The neutron dose rate measurements were made using a Tracerlab "Snoopy" neutron dose rate meter. A scaler was also used with the Snoopy to improve the low level measurements.

The calculated dose rates are based on the neutron leakage given by six-group, two-dimensional diffusion calculations; these diffusion and shielding calculations are discussed in Appendices D and E of the FBBF license application. Measured and calculated dose rates are presented in Table 6-1. The neutron dose rate at the side of the FBBF (inside of the shielding) was calculated using the neutron leakage with flux-to-dose-rate conversion factors recommended by the American Nuclear Society Shielding Standards Committee. The neutron dose rate at the top of the FBBF (inside the shielding) was calculated using fluxes from a twenty-one-group, two-dimensional diffusion calculation.

Two conclusions are drawn from the values given in the table:

1. --The two-dimensional diffusion calculations appear to underpredict the neutron leakage from the FBBF and/or to predict a too soft leakage energy spectrum.

2. --The measured and calculated effectiveness of the shielding are in relatively good agreement.

Attempts to measure the dose rates in the lecture hall and the lecture preparation room above the FBBF met with little success because of their small values. This was expected; the FBBF license application stated "...dose rate in rooms 114 and 114A for the source of 10^{10} neutrons/sec will probably be much too low to be measured. The shielding calculations discussed in Appendix D will therefore be used to relate the dose rates in room 114 and 114A to the dose rate on top of the FBBF shield (the ceiling of room B28C). Measurements of dose rates near the shield can then be used to estimate the dose rates in rooms 114 and 114A."

Table 6-1

DOSE RATES

Location	Calculation (mrem/hr)		Net Measurement		Measurement/ Calculation (ratio)	
Top of FBBF (radius 33 cm)	850	n[+]	1800	n	2.1	n
Side of FBBF	74	n	180	n	2.4	n
	< 1	g				
Top Shield Point	0.0053	n	0.0097	n	1.8	n
	0.018	g	0.018	g	1.0	g
	0.011	total	0.028	total	1.2	total
Side Shield Point	0.0025	g	0.0042	n	1.7	n
	0.0086	g	0.0058	g	0.7	g
	0.011	total	0.010	total	0.9	total
Preparation Room[*]	0.00061	total	0.0012	g[++]	2.0	total
Leacture Area[*]	0.00059	total	0.0006	g[++]	1.0	total
Seating Area[*]	0.000013	total	not detectable		--	

[*]Maximum calculated and measured values for area.

[+]Neutron dose rate indicated by n, gamma-ray dose rate indicated by g.

[++]Neutron dose rate not detectable.

7

EXPERIMENTAL MEASUREMENTS

The experimental measurements for determining the nuclear properties of blankets investigated in the FBBF facility can be divided into three broad catagories. In the first catagory are the integral reaction rate measurements including both neutron capture and fission rates. The second type of measurement is the determination of neutron energy spectra using proton-recoil proportional counters. The last catagory of measurements is the determination of the gamma-ray energy deposition throughout the blanket using thermoluminscent (TLD) dosimeters. Each of the three types of measurements can be compared with calculated results to provide a test of the calculational methods and input data that will be used to predict the performance of blankets in liquid metal fast breeder reactors.

INTEGRAL REACTION RATE MEASUREMENTS
(G.A. Harms, H.P. Chou, R.H.Johnson, and F.M. Clikeman)

Computer codes used to predict the neutron performance of blankets all calculate integral reaction rates such as the U-238 neutron capture rate and the U-238, U-235, and Pu-239 fission rate. Therefore, measurements of these integral reaction rates can provide a good test of the accuracy of the predicted values. In addition, further tests of the accuracy of the calculational methods can be provided if additional neutron capture reaction rates such as gold, manganese, molybdenum, indium, sodium and chlorine and fission rates such as Np-237 and Th-232 are also calculated and compared with experimental measurements. The comparison of all these reaction rates as a function of position in the blanket regions of the FBBF facility will thus provide a good test for the accuracy of the calculational methods and input data. If disagreement between the measurements and calculated values do occur, the use of such widely diverent cross sections should provide a good indication as to whether the disagreement arises in the input cross section data or is inherent in the basic assumptions underlying the calculations. The measured experimental reaction rates can also be used as input data for computer codes such as, CRYSTAL BALL, and SAND-II, which are used to experimentally determine neutron reaction rate spectra.

REPRODUCIBILITY OF FOIL ACTIVATION DATA

Because of the relatively low level of the neutron flux in the FBBF facility, especially in the outer regions of the blanket-reflector interface, the counting statistics from single activation measurements frequently do not have the precision required for meaningful comparisons between experimental and calculated results. In order to reduce the uncertainty in the experimental measurement it was important to establish the fact that the data from different experimental runs exposed at the same location, can be added together. Two experiments were performed to verify that data from different foils, activated at different times but in the same position, could be added together.

The first experiment was performed using the $^{55}Mn(n,\gamma)^{56}Mn$ reaction. The foils were activated at various times up to twenty-four hours and counted for approximately two half lifes or five hours. The experiment proceeded over a two week period at several different locations in the blanket regions of the FBBF facility. The measured activuties of the foils were corrected for irradiation time, decay of the activity following removal from the FBBF facility, and decay of the californium source to yield a saturated activity based upon a neutron source strength of 10^{10} neutrons per second. The results are shown in Fig. 7-1. Analysis of the distribution of the data points about the mean values are consistant with a standard deviation from the manganese experiments of about 2%.

A second test of the reproducibility of the data was performed using indium foils. A series of 21 irradiations were made in the same position (radius 26.6 cm) over a period of three days. Figure 7-2 presents the results of these experiments. The data are plotted with one standard deviation error bars derived from the counting statistics. For these measurements the standard deviation was 0.85%. The average indium activity is indicated by the dashed line. Five of the 21 measurements fall more than one standard deviation away from the average value; two of these values fall more than two standard deviation away from the average. These distribution data points are consistant with statistical predicitions. A chi-square analysis of the data gave a value of chi-square equal to 20 with probability of chi-square being exceeded by another experiment being equal to 0.45. Thus, it may be concluded that random errors in the data introduced by factors other than the counting statistics are small and that the data from several foil irradiations may be added together to improve the precision of the measurements.

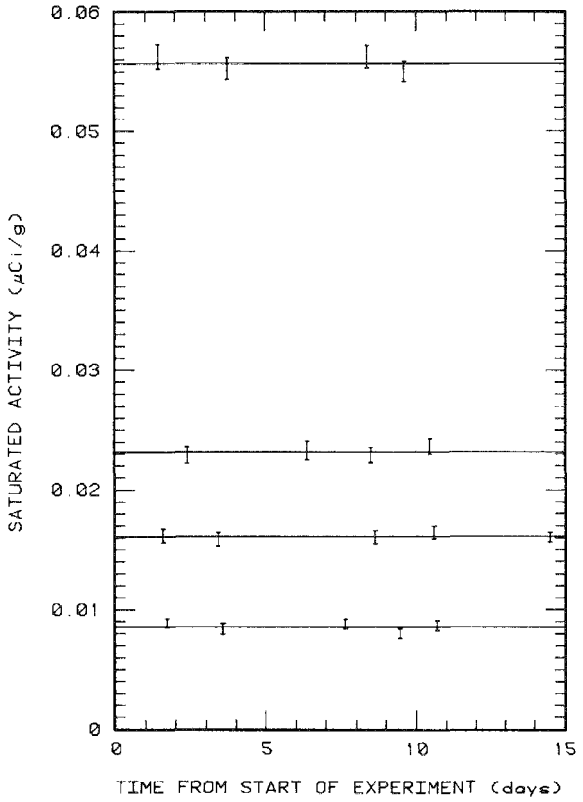

Figure 7-1: Reproducibility test of the FBBF using manganese foils. The solid lines indicate the average activity at each position. The measurements were taken radially at 23.7 cm, 50.3 cm, 56.3 cm, and 71.1 cm (top to bottom) from the centerline of the facility. The error bars represent counting statistics at the 90% confidence level.

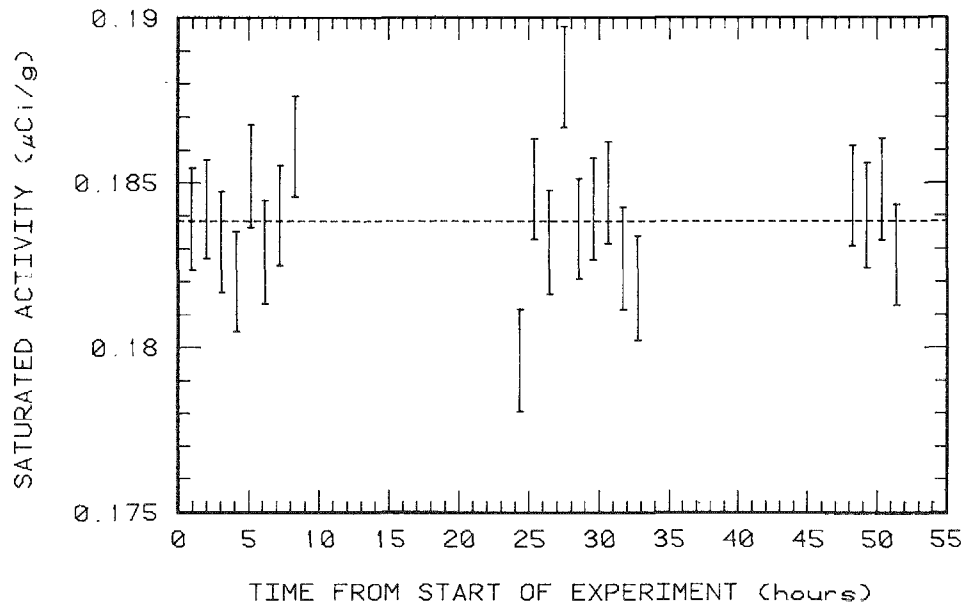

Figure 7-2: Integral capture measurements for indium-115 as a function of time for position A.2. The error bars are at one standard deviation.

INTEGRAL REACTION RATES MEASUREMENTS MADE AS A FUNCTION OF RADIAL DISTANCE

The FBBF blanket region is divided into 60° sections, each of which contains either 19 or 33 positions filled by removable experimental fuel rods. Figure 7-3 is a diagram of one sector showing all 33 experimental positions and the numbering system used to designate them. The sectors are lettered A through F, with the sectors A and D, at 180° from each other, containing the full 33 experimental positions while the other four sectors have only the azimuthal positions. Listed in Table 7-1 are the radial and azimuthal positions for the 33 experimenal locations available within a sector.

Foils to be irradiated in the FBBF are placed in thin metal covers (aluminum, cadmium, or stainless steel) and the foil cover assembly is placed between two UO_2 pellets in an experimental rod. The experimental rod is then placed in one of the positions. Each of the experiments are then irradiated for an optium time determined by such factors as the half life or the optium fission track density in the case of the fission reactions.

The experimental rods are then removed and the foils or fission track recorders are then counted. In the case of the activation foils the activity is determined either by a large lithium drifted germanium detector (GeLi) or a well type sodium iodide detector. The solid state fission track recorders are counted using an automated scanning optical microscope. The absolute activity of a foil is then determined and is corrected for the decay time, time of irradiation in the FBBF facility, and californium-252 source strength to determine an absolute reaction rate. Figures 7-4, 7-5 and 7-6 show typical preliminary reaction rates as a function of radial position that have been achieved with the FBBF facility. In all cases the activities have been plotted as 2π times the radius times the absolute saturated activity; this scale factor tends to remove the radial dependence and to emphasize the spectral dependence of the measured reaction rates. The results for the activation of gold, shown in Fig. 7-4, have a relative uncertainty of 0.3%. This uncertainty arises only from the counting statistics and does not include corrections for the uncertainty in the detector efficiency and the californium source. Together the uncertainties would lead to an over all uncertainty of about 3.5%, due mainly to the uncertainty in the absolute fission rate of the californium-252. Figure 7-5 shows similar results for the activation of manganese with a relative uncertainty of 1.3% in the counting statistics. Figure 7-6 shows the activity from neptunium-239 arising from a neutron capture in

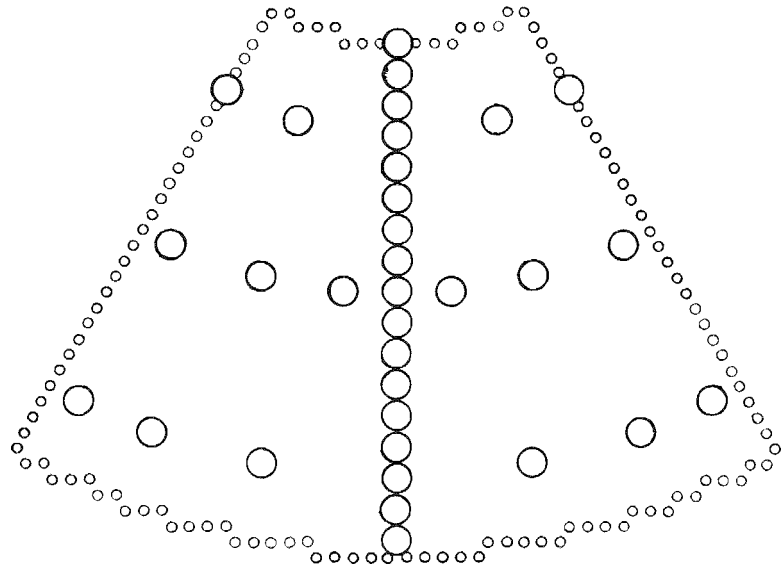

Figure 7-3 : Radial and azimuthal positions.

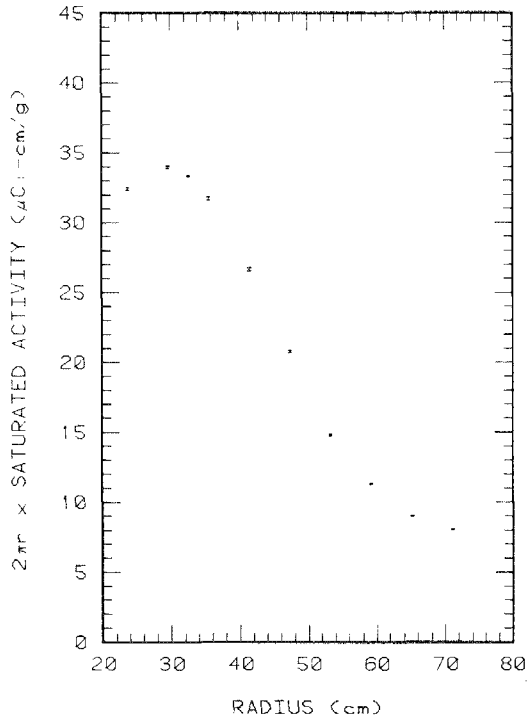

Figure 7-4 : 2π x radius x saturated activity of integral gold neutron capture rate as a function of positions in the radial blanket of the FBBF facility. The experimental error bars are one standard deviation based only on the counting statistics.

Table 7-1

RADIAL AND AZIMUTHAL POSITIONS

Position	Radial Location (cm)	Azimuthal Location off center (degrees)
1	23.69	0
2	26.65	0
3	29.61	0
4	32.57	0
5	35.53	0
6	28.49	0
7	41.45	0
8	44.41	0
9	47.37	0
10	50.33	0
11	53.29	0
12	56.26	0
13	59.22	0
14	62.18	0
15	65.14	0
16	68.10	0
17	71.06	0
21	32.48	30
22	32.48	16.83
23	32.48	16.83
24	32.48	30
31	47.96	26.46
32	47.65	15.61
33	47.65	6.18
34	47.65	6.18
35	47.65	15.61
36	47.96	26.46
41	65.03	27.39
42	64.94	20.82
43	64.94	11.39
44	64.94	20.82
45	64.94	27.39
46	65.03	

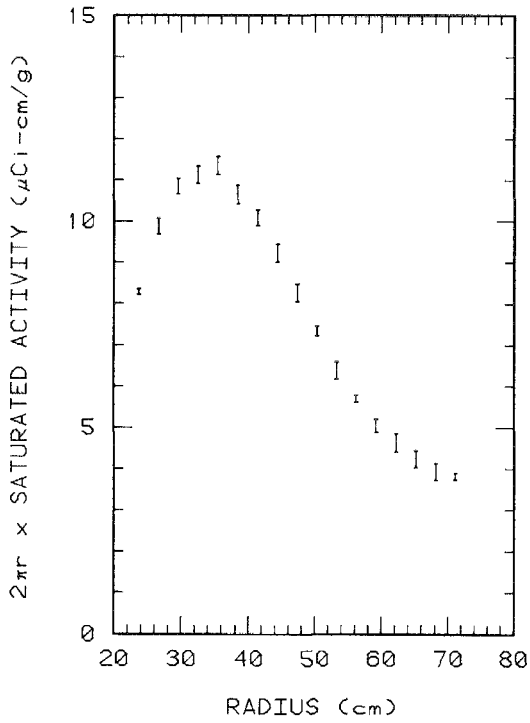

Figure 7-5: 2π x radius x saturated activity of the integral manganese neutron capture rate as a function of position in the radial blanket of the FBBF facility. The experimental error bars are one standard deviation based only on the counting statistics.

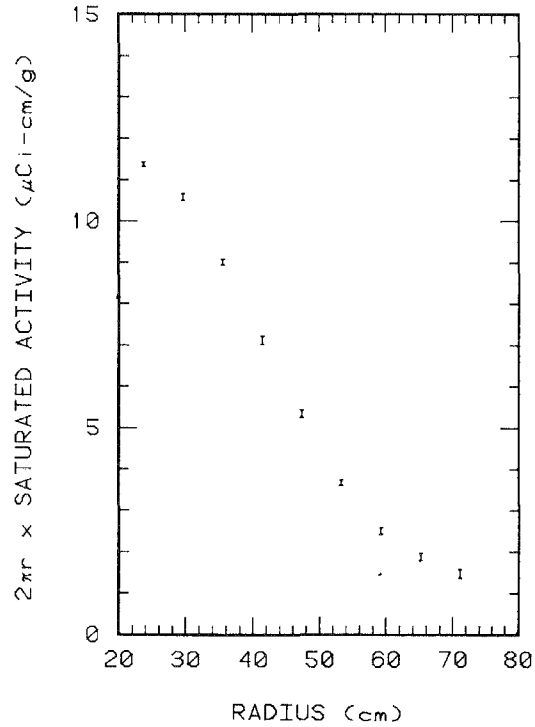

Figure 7-6 : 2π x radius x saturated activity of Np-239 produced by neutron capture in U-298 as a function of position in the radial blanket of the FBBF facility. The experimental error bars are one standard deviation based only on counting statistics.

238U Near the core blanket interface, at a distance approximately 22 cm, the counting statistics give a standard deviation of about 1%. Further out in the blanket near the blanket-reflector interface the standard deviation is about 5%. Both of these numbers are well within the uncertainties shown to be necessary for meaningful comparisons between calculated and experimental results.

These three integral reaction rate measurements demonstrate the capability of the FBBF for making integral measurements for comparison with calculated reaction rates. Additional integral reaction rate measurements including neutron capture in sodium, chlorine, and molybdenum will be made. And in addition integral fission rate measurements of Np-237, Th-232, U-235, U-238 and Pu-239 will be made.

NEUTRON SPECTRUM DETERMINATION USING PROTON-RECOIL METHODS
(D. W. Vehar and F. M. Clikeman)

One of the key measurements to be made in the blanket regions of the FBBF is the determination of the neutron spectra as a function of radial position. The primary method of measurement will be the use of proton-recoil detectors in which the fast neutrons impinge upon hydrogen in the detector and the corresponding proton energy distribution is measured. The proton energy distribution is then unfolded to yield the neutron energy spectra. By using two or more proton recoil detectors, filled either with hydrogen or methane, and several operating voltages for each detector, the neutron energy spectrum ranging from 1 keV to 2 MeV can be determined. The technique was developed by E. Bennett (34) at the Argonne National Laboratory and has been used extensively at Argonne. The technique has also been used at Purdue University since 1969 and several improvements, primarily in the areas of gamma-ray discrimination and energy calibration of the detectors, have been developed. Figure VII-7 shows a typical neutron spectrum measured in the blanket region of the FBBF facility. Future work will include measurement of the neutron spectrum as a function of both radius and axial height in the blanket with the measured neutron spectra compared with calculated spectra at various locations. The measured neutron spectra will also be used together with group cross sections derived from ENDF/B-IV cross section sets to calculate integral reaction rates which in turn will also be compared with measured integral reaction rates as previously described. This type of comparison should give valuable information as to the validity of the cross section sets being used in the calculations.

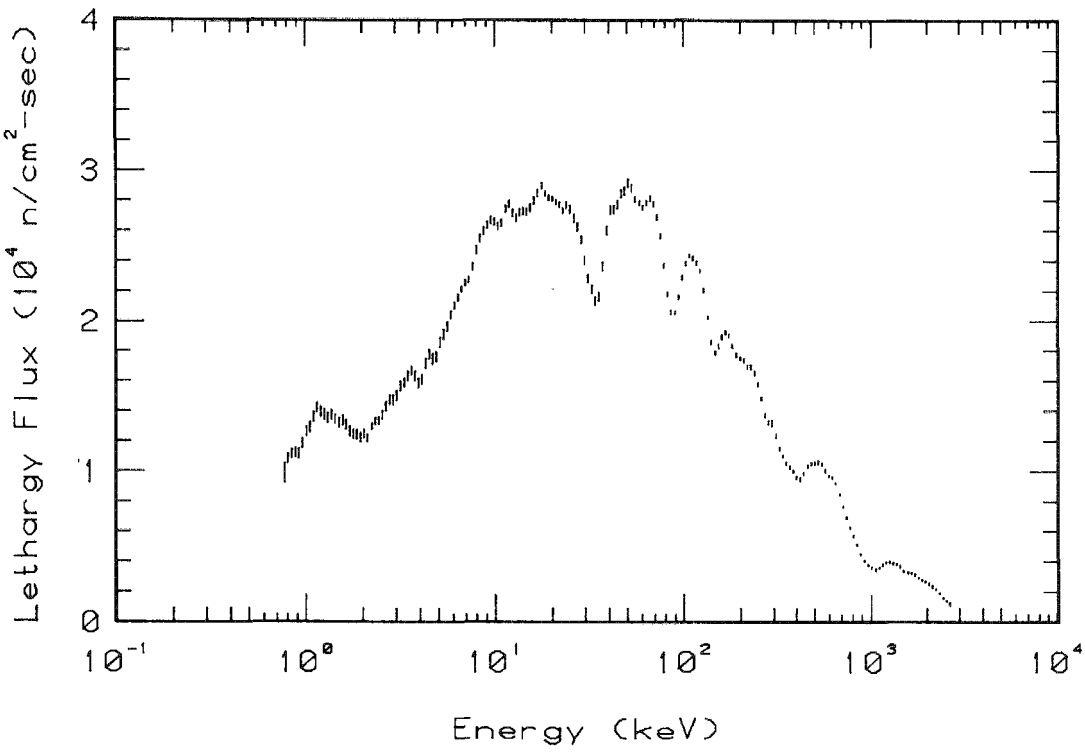

Figure 7-7: Neutron spectrum measured at a radial distance of 56 cm using proton recoil proportional counting technique. Three detectors, two filled with hydrogen and one with methane, were used in the measurement. The error bars represent one standard deviation and are based on the counting statistics in the proton spectrum. The effects of resonances in aluminum at 35, 90, and 150 keV and in oxygen at 440 keV and 1 MeV are clearly seen.

GAMMA-RAY DOSIMETRY MEASUREMENTS
(K. R. Koch and F. M. Clikeman)

Gamma-ray dosimetry measurements throughout the blanket regions of the FBBF are being made using CaF_2:Dy thermoluminscent dosimeters (TLD's). The gamma-ray absorption measurements using the TLD's will be used to determine the gamma-ray heating rate throughout the blankets used in the FBBF. The CaF_2:Dy TLD's were chosen because of their relatively low response to neutrons, long fading time characteristics and high atomic number. Reproducibility of TLD measurements, especially with the dosimeters as they are received from the supplier, are not precise enough to yield results that will give meaningful comparison with calculated values of the gamma heating rates. Therefore, the first step in the TLD measurements was to group the TLD dosimeters into precision sets for greater accuracy (35). In addition four TLD measurements are made at each location in the blanket and the results are combined. By using this method, reproducibility with

a standard deviation less than 1% can be achieved. Corrections for the background from the natural radioactivity of the uranium fuel are made by making measurements with the neutron source in the storage cask. The TLD's are exposed in the FBBF facility by placing them either in a stainless steel or lead holders. Corrections must then be made for the response of TLD's to the gamma-rays interacting in the holder. Solid state ionization theory (cavity theory) is being used to correct for the different electron spectra produced in the covers or sleeves holding the TLD's. The correction is applied as an f-factor which is defined as the ratio of the dose in the TLD to the sleeve dose. This allows for the dose determination in the material used in the TLD holder. The f-factors as a function of gamma-ray energy have been obtained from Simons (36) using the TERC/III code. An average f-factor is calculated at each radial position using calculated gamma-ray energy spectra and energy absorption coefficients. A preliminary set of TLD measurements using a lead holder are shown in Fig. 7-8 . Again the response is multiplied by 2π times radius. These preliminary results have not been normalized to an absolute source strength and therefore show only the relative gamma-ray heating measurements as a function of radius. Additional corrections for both the neutron response and the absolute gamma-ray response will also have to be made before the results can be compared with the calculated gamma heating rates.

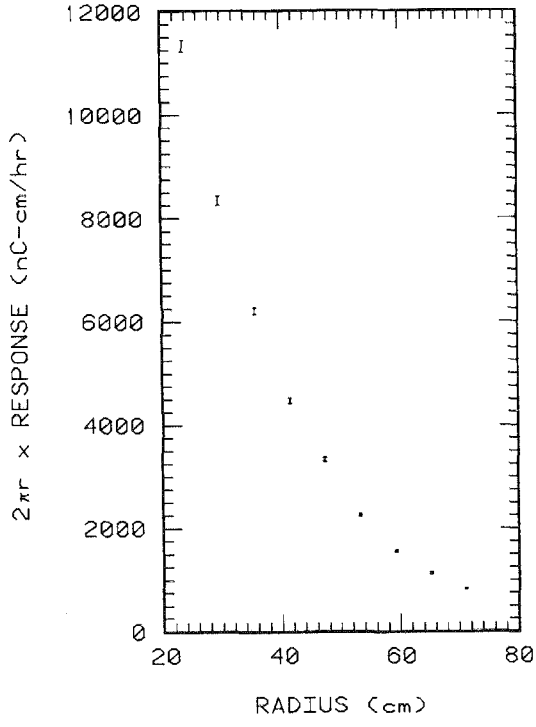

Figure 7-8 : 2π x radius x TLD response as a function of position in the radial blanket of the FBBF facility. The error bars represent one standard deviation based on the uncertainties that had been previously determined for the set of TLD dosimeters.

REFERENCES

1. W.G. Davey, "The Demonstration Reactor Benchmark Program," National Topical Meeting on New Developments in Reactor Physics and Shielding, Sept. 12-15, 1972, CONF-720901, Book 2, page 789 (Sept. 1972).

2. D. Meneghetti and W.B. Loewenstein, "Physics-Oriented Design Considerations of EBR-II," Trans. Amer. Nucl. Soc., 16, 275 (June 1973).

3. P.L. Hoffman, "FTR Neutronics: Status, Problems and Development Programs," National Topical Meeting on New Developments in Reactor Physics and Shielding, Sept. 12-15, 1972, CONF-720901, Book 2, Page 839 (Sept. 1972).

4. D.D. Freeman, P. Greebler, L.D. Noble and G.R. Pflasterer, "SEFOR: Verification of the Doppler Transient Shutdown Capability of LMFBR's," National Topical Meeting on New Developments in Reactor Physics and Shielding, Sept. 12-15, 1972, CONF-720901, Book 2, Page 986, (Sept. 1972).

5. B.J. Toppel, A.L. Rago and D.M. O'Shea, "MC^2, A Code to Calculate Multigroup Cross Section," ANL-7318, Argonne National Laboratory (1967).

6. H. Henryson, II, et al, "A User's Manual for the Intermediate-Group Spatially Dependent Multigroup Cross-Section Capability, SDX," FRA-TM-33, Argonne National Laboratory (1972).

7. P.I. Ammundson, et al, "Spatially Dependent Benchmark Parameters in the Initial Demonstration Plant Critical Assembly," National Topical Meeting on New Developments in Reactor Physics and Shielding, Sept. 12-15, 1972, CONF-720901, Book 2, Page 809 (Sept. 1972).

8. B.R. Sehgal and D. Meneghetti, "Analysis of Dosimetry Measurements in EBR-II, and EBR-II ZPR-3 Critical," American Nuclear Society Topical Meeting on the Irradiation Experimentation in Fast Reactors, Sept. 10-12, 1973, Page 355.

9. G.G. Simons, "Thermoluminescent Dosimetry Applied to Gamma-Ray Dose Measurements in Critical Assemblies," Applied Physics Division Annual Report, July 1, 1969 to June 30, 1970, ANL-7710, pp. 157-167, Argonne National Laboratory.

10. D. Meneghetti and W.B. Loewenstein, "EBR-II Irradiation Physics," National Topical Meeting on New Developments in Reactor Physics and Shielding, Sept. 12-15, 1972, CONF-720901, Book 2, Page 906 (Sept. 1972).

11. K.O. Ott and C.W. Terrell, "Subcritical Fast Reactor as a University Research Facility," Trans. Am. Nucl. Soc. 13, 456 (1970).

12. K.O. Ott, K.R. Boldt, and F.M. Clikeman, "Review of Nuclear Physics Uncertainties in Fast Reactor Blankets," Purdue University, PNE-75-103 (Mar 1975).

13. K.R. Boldt, "Preliminary Analysis of the FBBF Experiment to Determine Uranium-238 Capture Rates by the Detection of Neptunium-239 Decays," Purdue University, M.S. Thesis (Dec. 1976).

14. F.G. Krauss, K.O. Ott and F.M. Clikeman, "The Conceptural Design of a Fast Subcritical Blanket Facility," Nucl. Tech. 25, 429, (1975).

15. "Clinch River Breeder Reactor Plant," Reference Design Report, Vol. 1, Advanced Reactor Division, Westinghouse Electric Corporation, June 1974.

16. D.J. Malloy, L.B. Luck and G.L. Terpstra, "LAZARUS, A 1-Dimensional Diffusion Theory Package for Fast Reactor Calculations," Purdue Universtiy, PNE-75-112 (1976).

17. FBBF Quarterly Progress Report for the Period July 1, 1977 - September 31, 1977, Purdue University PNE-77-120 (COO-2826-5) (1977).

18. R.G. Soltesz and R.K. Disney, "Nuclear Rocket Shielding Methods, Modification, Updating, and Input Data Preparation, Volume 4 -- One-Dimensional, Discrete Ordinates Transport Technique," Westinghouse Astronuclear Laboratory, WANL-PR-(LL)-034 (1970).

19. "DLC-37/EPR, Coupled 100-Group Neutron 21-Group Gamma-Ray Cross Sections for EPR Neutronics," Radiation Shielding Information Center, Oak Ridge National Laboratory.

20. W.E. Ford, III, R.T. Santoro, R.W. Roussin, and D.M. Plaster, "Modification Number One to the Coupled 100n21γ Cross Section Library for EPR Calculations," Oak Ridge National Laboratory, ORNL/TM-5249 (1976).

21. FBBF Quarterly Progress Report for the Period, July 1, 1977 - September 30, 1977, pp. 24-25, Purdue Universtiy, PNE-77-120 (COO-2826-5) (1977).

22. FBBF Quarterly Progress Report for the Period July 1, 1977 - September 30, 1977, pp. 5-7, Purdue University, PNE-77-120 (COO-2826-5), (1977).

23. FBBF Quarterly Progress Report for the Period, October 1, 1977 - December 31, 1977, Purdue University, PNE-78-123, (COO-2826-6), (1978).

24. Fast Breeder Blanket Facility Quarterly Progress Report for the Period January 1, 1976 to August 30, 1976. Edited by K.O. Ott, PNE-76-115, COO-2826-1, Purdue University, West Lafayette, Indiana.

25. Fast Breeder Blanket Facility Quarterly Progress Report for the Period September 1, 1976 to December 31, 1976. Edited by K.O. Ott, PNE-76-116, COO-2826-2, Purdue University, West Lafayette, Indiana.

26. Fast Breeder Blanket Facility Quarterly Progress Report for the Period January 1, 1977 to March 31, 1977. Edited by K.O. Ott, PNE-77-119, COO-2826-4, Purdue University, West Lafayette, Indiana.

27. Fast Breeder Blanket Facility Quarterly Progress Report for the Period April 1, 1977 to June 30, 1977. Edited by K.O. Ott, PNE-77-119, COO-2826-4, Purdue University, West Lafayette, Indiana.

28. Fast Breeder Blanket Facility Quarterly Progress Report for the Period October 1, 1977 to December 31, 1977. Edited by K.O. Ott, PNE-78-121, COO-2826-6, Purdue University, West Lafayette, Indiana.

29. Fast Breeder Blanket Facility Quarterly Progress Report for the Period April 1, 1978 to June 30, 1978. Edited by F.M. Clikeman PNE-78-132, COO-2826-9, Purdue University, West Lafayette, Indiana.

30. R.C. Borg, "Fast Breeder Blanket Facility (FBBF) Safety Calculation for the Period January 1, 1976 to September 30, 1978," PNE-78-135, Purdue University, West Lafayette, Indiana.

31. H.P. Flatt, "The FOG One-dimensional Neutron Diffusion Equation Codes," NAA-SR-6104.

32. W.W. Little, Jr. and R.W. Hardie, "2DB, A Two-Dimensional Diffusion Burnup Code for Fast Reactor Analysis," Battelle Pacific Northwest Laboratories, BNWL-460 (1968).

33. J. E. Suich and H. C. Honeck, "The Hammer System, Heterogeneous Analysis by Multigroup Methods of Exponentials and Reactors." Savannah River Laboratory, DP-1064 (January 1967).

34. E.F. Bennet and T.J. Yule, "Techniques and Analysis of Fast Neutron Sepctroscopy Proton-Recoil Proportional Counters," ANL-7753, (August 1971).

35. G.G. Simons and T.S. Huntsman, "Precision of ^{7}LiF Thermoluminescent Dosimeters Using Sensitivity Selection," Argonne National Laboartory ZPR-TM-200 (1975).

36. G.G. Simons, Private Communication.